

## 6. Bohm Trajectories and the Tunneling Time Problem

C.R. Leavens and G.C. Aers

With 21 Figures

Although many approaches based on conventional interpretations of quantum mechanics have been developed for calculating the average time taken for an electron to tunnel through a potential barrier, a satisfactory solution remains elusive. These approaches are discussed very briefly, focussing on the question of whether the concept of ‘tunneling time’ or, more generally, ‘mean transmission time’ is a meaningful one. Then it is shown that Bohm’s causal or trajectory interpretation provides a well-defined and unambiguous prescription for calculating transmission times that are conceptually meaningful *within that interpretation*. Results of such calculations are presented for single and double rectangular barriers. The time-modulated rectangular barrier is treated in detail to emphasize the importance of considering distributions of transmission and reflection times and not just the mean transmission time. Finally, the possibility of determining tunneling times experimentally is discussed.

### 6.1 Background

#### 6.1.1 Motivation

In the theoretical analysis of a complex dynamical system, comparison of the various time scales involved often motivates and/or justifies useful approximations. When tunneling through a potential barrier plays a key role it is often assumed that the average time for an electron to tunnel through the barrier, i.e. the tunneling time  $\tau_T$ , is an important time scale. In the field of scanning tunneling microscopy, such an assumption has been made in investigations of the dynamical image potential [6.1, 2], the generation of d.c. current by laser illumination of the tip–sample junction [6.3, 4], the anomalously low barrier for tunneling through aqueous solutions [6.5], and the effect of atomic vibrations on image resolution [6.6]. The tunneling time of interest in the above context is an intrinsic property, i.e. a property of the undisturbed system. If an external clock were coupled to the system to ‘measure’  $\tau_T$  directly then the observed tunneling time might be so strongly perturbed by interaction with the measuring apparatus as to be of little use in the comparison of relevant time scales for the unperturbed system. Proceeding indirectly by using the dynamics of the undisturbed system as an internal clock, one might infer the order of magnitude of the

intrinsic tunneling time by the success of approximations based on its magnitude relative to the other time scales. This would involve comparison of the approximate results with accurate experimental or theoretical ones. However, one should bear in mind that the most basic quantities are the transmission and reflection time *distributions* not just their average values. One should not automatically assume for any phenomenon involving tunneling that the average transmission time is the relevant time scale nor, for that matter, that the entire width of the barrier is the only length scale of importance in determining the temporal characteristics. With this in mind we adopt a more general point of view in the following.

### 6.1.2 Defining the Problem

To define the quantities of interest in the ‘tunneling time problem’ [6.7–12] consider an ensemble of scattering experiments in each of which an electron with the same initial wave function  $\psi(z, t = 0)$  is incident normally from the left on the potential barrier  $V(r, t) = V(z, t)\theta(z)\theta(d - z)$  which varies only in the  $z$  direction.<sup>1</sup> The mean transmission time  $\tau_T(z_1, z_2)$  is defined as the average time spent in the region  $z_1 \leq z \leq z_2$  subsequent to  $t = 0$  by those electrons that are ultimately transmitted. Only a fraction of the ensemble members, equal to the transmission probability  $|T|^2$ , are involved in the average determining  $\tau_T$ . The corresponding mean reflection time  $\tau_R(z_1, z_2)$  is defined as the average time spent in the region  $z_1 \leq z \leq z_2$  by those electrons that are ultimately reflected and involves only the remaining fraction  $|R|^2 \equiv 1 - |T|^2$  of the ensemble members. Finally, the mean dwell time  $\tau_D(z_1, z_2)$  is the average time spent between  $z_1$  and  $z_2$  by an electron irrespective of whether it is eventually transmitted or reflected. Clearly, since  $\tau_D$  involves all members of the ensemble, the relation

$$\tau_D(z_1, z_2) = |T|^2 \tau_T(z_1, z_2) + |R|^2 \tau_R(z_1, z_2) \quad (6.1)$$

must hold. Although the positions  $z_1$  and  $z_2$  are arbitrary, except for the restriction  $z_1 \leq z_2$ , the case of usual interest is  $z_1 = 0$  and  $z_2 = d$  for the abrupt barriers considered here. The so-called ‘tunneling time’ or ‘traversal time’ is then the quantity  $\tau_T(0, d)$ . Strictly speaking, the former term should be used only when the wave-packet and barrier parameters are such that over-the-barrier propagation makes a negligible contribution to the transmission probability. Moreover, for sloping rather than abrupt barriers the classical turning points depend on energy and the spatial extent of the tunneling region is consequently blurred for a wave packet with finite energy width. Hence, the phrase ‘tunneling time’ will usually be avoided in the remainder of this chapter.

---

<sup>1</sup> It should be emphasized that in this chapter we do not consider the related and much better understood problem of the escape time for a particle prepared in a metastable state of a potential well.

The mean transmission time  $\tau_T(z_1, z_2)$  was defined in words rather than by a mathematical expression, e.g. the expectation value of a Hermitean operator  $\hat{\tau}_T(z_1, z_2)$ , essentially because in quantum mechanics time is regarded as a parameter or c-number, not as a dynamical observable represented by such an operator. Hence, there is no automatic prescription in the basic formalism for calculating  $\tau_T$  and the other characteristic times  $\tau_R$  and  $\tau_D$ . One might therefore ask if these quantities are meaningful concepts. It has been argued [6.13] that they are not because they imply the existence of microscopically well-defined particle trajectories. The latter concept is, of course, expressly forbidden in conventional interpretations because it is impossible, even in principle, to observe such a trajectory due to the position-momentum uncertainty relation. Another argument [6.13] against transmission and reflection times being meaningful is that, within conventional interpretations, it is impossible to divide the probability density  $|\psi(z, t)|^2$  inside the barrier into ‘to be transmitted’ and ‘to be reflected’ components. In our opinion, as discussed in the next section, this negative response to the above question is at least a consistent one. On the other hand, within *Bohm’s* causal or trajectory interpretation of quantum mechanics [6.14–16] the notion of a precisely well-defined particle trajectory is not only a meaningful concept but a central one. Moreover, it is possible to divide  $|\psi(z, t)|^2$  inside the barrier into ‘to be transmitted’ and ‘to be reflected’ components. Consequently, as discussed in Sect. 6.3, Bohm’s interpretation leads to a unique, well-defined prescription for calculating meaningful transmission, reflection and dwell times. This prescription is applied to a number of simple systems in Sect. 6.4. Finally, in Sect. 6.5, the problem of experimentally determining mean transmission and reflection times is discussed from the Bohm trajectory and conventional points of view.

## 6.2 A Brief Discussion of Previous Approaches

Since all of the theoretical results for  $\tau_T$  and  $\tau_R$  discussed in this section can be simply related to those obtained with *Feynman* path integral techniques [6.17] by *Sokolovski* and coworkers [6.18–20] we focus on their approach. The starting point is the classical expression

$$t^{cl}[z_1, z_2; z(t)] = \int_0^\infty dt \theta[z(t) - z_1] \theta[z_2 - z(t)] \quad (6.2)$$

for the time spent subsequent to  $t = 0$  in the region  $z_1 \leq z \leq z_2$  by a point particle following its classical trajectory  $z(t)$ . They generalize this expression for the dwell time to the quantum regime by replacing  $z(t)$  in the above functional by a Feynman path  $z(\bullet)$  and then averaging over all such paths according to the Feynman prescription, i.e.

$$\tau_D(z_1, z_2) = \langle \psi^*(z', t_\infty) t^{cl}[z_1, z_2; z(\bullet)] \psi(z, 0) \rangle_F / \langle \psi^*(z', t_\infty) \psi(z, 0) \rangle_F . \quad (6.3)$$

Here  $\langle \dots \rangle_F$  denotes an average with weight factor  $\exp[iS(z(\bullet))/\hbar]$  over all paths  $z(\bullet)$  joining the space-time points  $(z, 0)$  and  $(z', t_\infty)$  followed by an average over all  $z$  and  $z'$ .  $S[z(\bullet)]$  is the classical action and the time  $t_\infty$  must be large enough that the scattering process is essentially complete. Evaluation of (6.3) leads to the real, non-negative quantity

$$\tau_D(z_1, z_2) = \int_0^\infty dt \int_{z_1}^{z_2} dz |\psi(z, t)|^2 , \quad (6.4)$$

which many, including the present authors, regard as the only firm result in the field. For the special case of an ‘incident’ plane-wave  $\exp(ikz)$  of wavenumber  $k$  it can be shown [6.21] that (6.4) becomes

$$\tau_D(k; z_1, z_2) = \frac{1}{j_k^{(i)}} \int_{z_1}^{z_2} dz |\psi_k(z)|^2 , \quad (6.5)$$

a result first postulated by Büttiker [6.22]. Here  $j_k^{(i)} = \hbar k/m$  is the incident probability current density and  $\psi_k(z)$  is the stationary-state wave function.

At sufficiently large times  $t_\infty$  the wave function can be written to a very good approximation as the sum of reflected and transmitted components, i.e.  $\psi(z', t_\infty) = \psi_R(z', t_\infty) + \psi_T(z', t_\infty)$ . Based on this, Sokolovski and Connor [6.19] determine the mean transmission and reflection times  $\tau_T$  and  $\tau_R$  by replacing  $\psi^*(z', t_\infty)$  in (6.3) by  $\psi_T^*(z', t_\infty)$  and  $\psi_R^*(z', t_\infty)$ , respectively. The resulting expressions for  $\tau_T$  and  $\tau_R$  are, in general, complex-valued quantities. For an ‘incident’ plane-wave they take the simple form

$$\tau_T^{SB}(k; z_1, z_2) = i\hbar \int_{z_1}^{z_2} dz \frac{\delta \ln T(k)}{\delta V(z)} , \quad \tau_R^{SB}(k; z_1, z_2) = i\hbar \int_{z_1}^{z_2} dz \frac{\delta \ln R(k)}{\delta V(z)} , \quad (6.6)$$

derived by Sokolovski and Baskin [6.18]. Here  $T \equiv |T| \exp(i\phi_T)$  and  $R \equiv |R| \exp(i\phi_R)$  are the transmission and reflection probability amplitudes. The imaginary part of  $|T|^2 \tau_T^{SB} + |R|^2 \tau_R^{SB}$  is exactly zero and the real part is exactly equal to  $\tau_D$  so that the sum-rule (6.1) is satisfied [6.18]. For the special case of perfect transmission ( $|T|^2 = 1$ ) the transmission probability is stationary with respect to small changes in the barrier potential, i.e.  $\delta \ln |T|/\delta V(z) = 0$ . Hence, the imaginary part of  $\tau_T^{SB}$  is zero and  $\tau_T^{SB}$  is identical to the mean dwell time  $\tau_D$ . Similarly, for perfect reflection  $\tau_R^{SB} = \tau_D$ .

The real and (minus) the imaginary parts of  $\tau_T^{SB}(k; 0, d)$  are identical to the spin-precession traversal time of Rybachenko [6.23] and the spin-rotation traversal time of Büttiker [6.22] respectively. These are derived, following Baz' [6.24], from an analysis of the effect of an infinitesimal uniform magnetic field, confined to the barrier, on the components of the average spin per transmitted electron in the plane perpendicular to the field and in the field direction respectively. Neither of these traversal times can stand on its own: the former is essentially independent of the width  $d$  of an opaque rectangular barrier leading to a mean transmission speed that can exceed the speed of light  $c$  even in the

corresponding relativistic calculation [6.25]; the latter can be negative for above barrier transmission. Accordingly, Büttiker identified the actual traversal time with the square-root of the sum of their squares, i.e. with  $|\tau_T^{SB}(k; 0, d)|$ . This is referred to as the Larmor clock traversal time in the rest of this paper. It is identical to the *Büttiker–Landauer* traversal time derived by considering the sensitivity of  $T$  to the instantaneous height of a time-modulated barrier [6.26, 27]. For the special cases of perfect transmission and perfect reflection the spin-precession, Larmor clock and time-modulated barrier approaches all give the correct result (6.5) for  $\tau_T$  and  $\tau_R$  respectively.

When the derivation leading to  $\tau_T^{SB}$  is repeated, ignoring the interference between the incident and reflected components of the wave function, another complex quantity is obtained [6.19] that is closely related to other traversal times in the literature: its real part is identical to the phase time of *Bohm* [6.28] and *Wigner* [6.29] and to the spin-precession time of *Huang et al.* [6.30], while its imaginary part is the spin-rotation traversal time of the latter authors; its modulus is identical to the traversal time obtained by *Büttiker* and *Landauer* [6.31] from an analysis of the coherent transmission of two plane waves with slightly different energies. For the special case of perfect reflection, none of these approaches gives a mean reflection time that agrees with the result (6.5).

It is important to note that all of the above approaches are concerned with *intrinsic* transmission and reflection times because they are ultimately based on (6.2) which represents an ideal clock that ‘runs’ only when the electron is in the region of interest and does not perturb its motion in any way. Moreover, the fact that they do not all give the same answer to such an apparently simple problem as the dependence of  $\tau_T(k; 0, d)$  on the width  $d$  of an opaque rectangular barrier<sup>2</sup> should not be swept under the rug by claiming that they are concerned with different quantities from the outset.

It should also be emphasized that, under the right conditions, any one of the above times might be an important parameter. For example, if a tunneling experiment involves a very small constant change in the barrier height  $V(z)$  then there is no doubt that the relative sensitivity of the transmission probability amplitude to changes in average barrier height  $\bar{V}$ , i.e.  $\partial \ln T(k)/\partial \bar{V}$ , is a relevant quantity. If one chooses to multiply this complex-valued quantity by  $i\hbar$  then the resulting ‘time’ is obviously also relevant (whether it is the real part, imaginary part or modulus which is most important depends on the experimental situation). This however does not necessarily mean that the resulting time, which is identical to  $\tau_T^{SB}(k; 0, d)$  [6.8], should be identified with the actual mean transmission time.

Of more importance than the question of which, if either, of two different approaches is ‘better’ is the question of whether or not the concepts of transmission and reflection times are meaningful. The point of view that they are not is

---

<sup>2</sup> For example, the time-modulated barrier and spin-precession results for  $\tau_T(k; 0, d)$  are linear in  $d$  and independent of  $d$ , respectively.

consistent with the fact that there is no known approach based on conventional quantum mechanics which leads to real, non-negative transmission and reflection times that satisfy (6.1) and which does not lead to mean transmission speeds in excess of  $c$  [6.8]. Sokolovski and Connor [6.19] claim that, in general, transmission and reflection times must be complex valued and that it is misguided to search for a unique, well-defined prescription for calculating real-valued transmission and reflection times, particularly by invoking non-standard interpretations of quantum mechanics. We do not find their arguments compelling and in the next section explore the problem within an interpretation of quantum mechanics that leads naturally to transmission and reflection times satisfying the above criteria.

## 6.3 Bohm's Trajectory Interpretation of Quantum Mechanics

### 6.3.1 A Brief Introduction

In Bohm's interpretation of non-relativistic quantum mechanics [6.14–16], an electron is a particle the motion of which is causally determined by an objectively real complex-valued field  $\psi(z, t)$  so that it has a well-defined position and velocity at each instant of time. This is diametrically opposed to the fundamental tenets of conventional interpretations. Nevertheless, it is claimed that with three additional postulates, Bohm's interpretation leads to precisely the same results as the conventional ones for all experimentally observable quantities. These three postulates are: (1) the guiding field

$$\psi(z, t) \equiv R(z, t) \exp[iS(z, t)/\hbar] \quad (R \text{ and } S \text{ real}) \quad (6.7)$$

satisfies the time-dependent Schrödinger equation (TDSE)  $[i\hbar\partial/\partial t + (\hbar^2/2m)\partial^2/\partial z^2 - V(z, t)]\psi(z, t) = 0$ ; (2) the velocity of an electron located at the position  $z$  at time  $t$  is given by

$$v(z, t) = m^{-1} \partial S(z, t) / \partial z ; \quad (6.8)$$

(3)  $|\psi(z, t)|^2 dz$  is the probability of the electron *being* between  $z$  and  $z + dz$  at time  $t$  even in the absence of a position measurement. In conventional interpretations this quantity is the probability of the electron *being found* between  $z$  and  $z + dz$  at time  $t$  by a precise position measurement.

Substitution of (6.7) into the TDSE and separation of the resulting real and imaginary parts gives the modified Hamilton–Jacobi equation

$$\partial S(z, t) / \partial t + (2m)^{-1} [\partial S(z, t) / \partial z]^2 + V(z, t) + Q(z, t) = 0 \quad (6.9)$$

with

$$Q(z, t) \equiv -(\hbar^2/2m) R^{-1}(z, t) \partial^2 R(z, t) / \partial z^2 , \quad (6.10)$$

and the continuity equation

$$\partial P(z, t)/\partial t + \partial j(z, t)/\partial z = 0 \quad (6.11)$$

relating the probability and probability current densities

$$P(z, t) \equiv R^2(z, t) \equiv |\psi(z, t)|^2 , \quad (6.12)$$

$$j(z, t) \equiv P(z, t) v(z, t)$$

$$\equiv (\hbar/2im) [\psi^*(z, t) \partial\psi(z, t)/\partial z - \psi(z, t) \partial\psi^*(z, t)/\partial z] , \quad (6.13)$$

respectively. Bohm attributes the differences between quantum and classical mechanics mainly to the ‘quantum potential’  $Q$  and regards the classical limit as the limit in which  $Q$  is completely negligible compared with all other relevant energies. Since the differences between quantum and classical physics can be dramatic it should not come as a surprise that the quantum potential can have correspondingly remarkable properties. For example, since  $R(z, t)$  occurs in both the numerator and denominator of (6.10) it is possible for the quantum potential to have an important effect even in a region where  $|\psi(z, t)|^2$  is apparently negligible. The quantum potential has even more remarkable properties for many-electron systems: it can be non-local, the quantum potential acting on one electron being determined instantaneously at a distance by others in the system and not just through some unvarying function of particle positions but through the quantum state  $\Psi$  of the entire system. Non-locality is a necessary feature, according to *Bell’s theorem* [6.32], of any realistic interpretation of quantum mechanics, such as Bohm’s, which reproduces all the experimental consequences of the conventional interpretations.

Bohm’s quantum potential approach has provided fresh insight into measurement theory including the notorious collapse of the wave function which is not required in his interpretation [6.33, 34], the Einstein–Podolsky–Rosen thought experiment [6.35] and, returning to one-particle systems for a few more examples, the two-slit interference experiment [6.36], the Aharonov–Bohm effect [6.37], delayed-choice experiments [6.38], and quantum mechanical tunneling [6.39]. The following discussion of transmission, reflection and dwell times within Bohm’s interpretation is a natural and long overdue extension of the work of *Dewdney* and *Hiley* [6.39].

### 6.3.2 Transmission and Reflection Times Within Bohm’s Interpretation

Given the initial position  $z^{(0)} \equiv z(t = 0)$  of an electron with initial wave function  $\psi(z, t = 0)$ , its subsequent trajectory  $z(z^{(0)}, t)$  is uniquely determined by simultaneous integration of the TDSE and the guidance equation  $dz(t)/dt = v(z, t)$  given by (6.8). Alternatively, such trajectories can be obtained by simultaneous integration of the TDSE and Newton’s equation of motion with the usual potential energy  $V(z, t)$  augmented in the latter by the quantum potential

$Q(z, t)$ .<sup>3</sup> Now, suppose that two Bohm trajectories with the same guiding field  $\psi(z, t)$  intersect at the space-time point  $(z_i, t_i)$ . It follows immediately from  $v(z, t) = m^{-1} \partial S(z, t)/\partial z$  that both trajectories have the same velocity as well as the same position at time  $t_i$ . Since the time evolution of the trajectories is given by a second-order differential equation the two trajectories must then coincide at all times  $t > t_i$  in the future and, using time reversal invariance, at all times  $t < t_i$  in the past. Hence, Bohm trajectories do not intersect. This fact will be very useful in what follows.

The interpretation of a Bohm trajectory as an actual particle trajectory [6.14–16], rather than an abstract mathematical construct, immediately leads to a unique and well-defined prescription [6.40, 41] for calculating transmission and reflection times. For an electron that is at  $z = z^{(0)}$  at  $t = 0$  the time spent thereafter in the region  $z_1 \leq z \leq z_2$  is *unambiguously* given by replacing the classical trajectory in the right-hand-side of (6.2) by a Bohm trajectory, i.e.,

$$t(z^{(0)}; z_1, z_2) = \int_0^\infty dt \theta[z(z^{(0)}, t) - z_1] \theta[z_2 - z(z^{(0)}, t)] \quad (6.14)$$

In practice, the initial location  $z^{(0)}$  of an electron is not known exactly and uncertainty enters Bohm's deterministic theory through the postulated probability distribution  $P(z^{(0)}, 0) \equiv |\psi(z^{(0)}, 0)|^2$  for  $z^{(0)}$ . Proceeding as in classical statistical mechanics, the mean dwell time is then given by

$$\tau_D(z_1, z_2) \equiv \langle t(z^{(0)}; z_1, z_2) \rangle \quad (6.15)$$

where for any function  $f$  of  $z^{(0)}$

$$\langle f(z^{(0)}) \rangle \equiv \int_{-\infty}^{\infty} dz^{(0)} |\psi(z^{(0)}, 0)|^2 f(z^{(0)}) . \quad (6.16)$$

Insertion of an integral over all  $z$  of the delta function  $\delta[z - z(z^{(0)}, t)]$  into (6.15) immediately gives the equivalent, and perhaps intuitively obvious, result [6.40]

$$\tau_D(z_1, z_2) = \int_0^\infty dt \int_{z_1}^{z_2} dz |\psi(z, t)|^2 \quad (6.17)$$

with

$$|\psi(z, t)|^2 \equiv \langle \delta[z - z(z^{(0)}, t)] \rangle . \quad (6.18)$$

Equation (6.17) is precisely the result (6.4) derived using standard quantum mechanics by Sokolovski and Baskin [6.18].

---

<sup>3</sup> Although this method of calculation presumably could be more efficient, trajectories being calculated to order  $(\Delta t)^2$  rather than just  $\Delta t$ , it has not been attempted in our work because of possible complications resulting from the classical force  $-\partial V(z, t)/\partial z$  being singular at the edges of rectangular barriers.

In the following discussion of mean transmission and reflection times for finite wave packets, it is always assumed that the initial wave packet  $\psi(z, t = 0)$  is normalized to unity and is sufficiently far to the left of the barrier region  $0 \leq z \leq d$  that the initial probability density  $|\psi(z, t = 0)|^2$  is completely negligible for  $z \geq 0$ . In the calculations presented here, the centroid of the initial wave packet is usually chosen so that  $|\psi(z, t = 0)|^2$  integrated over the region  $0 \leq z \leq \infty$  is equal to  $10^{-4} |T|^2$ . Now, since Bohm trajectories do not intersect each other, there is a special starting point  $z_c^{(0)}$  given by

$$\int_{z_c^{(0)}}^{\infty} dz^{(0)} |\psi(z^{(0)}, 0)|^2 = |T|^2 \quad (6.19)$$

such that only those trajectories  $z(z^{(0)}, t)$  with  $z^{(0)} > z_c^{(0)}$  are ultimately transmitted contributing to  $|T|^2$  and only those with  $z^{(0)} < z_c^{(0)}$  are ultimately reflected contributing to  $|R|^2$ . Hence the mean transmission and reflection times are uniquely given by

$$\tau_T(z_1, z_2) = \langle t(z^{(0)}; z_1, z_2) \theta(z^{(0)} - z_c^{(0)}) \rangle / \langle \theta(z^{(0)} - z_c^{(0)}) \rangle , \quad (6.20)$$

$$\tau_R(z_1, z_2) = \langle t(z^{(0)}; z_1, z_2) \theta(z_c^{(0)} - z^{(0)}) \rangle / \langle \theta(z_c^{(0)} - z^{(0)}) \rangle , \quad (6.21)$$

where  $|T|^2 = \langle \theta(z^{(0)} - z_c^{(0)}) \rangle$  and  $|R|^2 = \langle \theta(z_c^{(0)} - z^{(0)}) \rangle$ . Obviously  $\tau_T$  and  $\tau_R$  are real-valued non-negative quantities and the sum-rule (6.1) is satisfied exactly.

The above prescription should be contrasted with the usual approaches based on the time evolution of the wave function [6.28, 29, 42–46] which assume that the centroid (or peak) of the incident probability density  $|\psi(z, 0)|^2$  evolves into the centroid (or peak) of the transmitted component  $|\psi_T(z, t_\infty)|^2$ . This assumption has no justification in conventional quantum mechanics as has been pointed out by *Büttiker* and *Landauer* [6.31]. Within Bohm's interpretation the assumption is simply incorrect because it is only that part of the initial wave packet to the right of  $z_c^{(0)}$  that evolves into the transmitted component. It should be noted that for any wave packet of finite spatial extent, the usual TDSE approaches lead to negative traversal times whenever the initial centroid is too far from the barrier [6.21].

Of more general interest than their mean values are the transmission and reflection time distributions [6.40, 41]

$$P_T[t(z_1, z_2)] \equiv \langle \theta(z^{(0)} - z_c^{(0)}) \delta[t(z_1, z_2) - t(z^{(0)}; z_1, z_2)] \rangle / \langle \theta(z^{(0)} - z_c^{(0)}) \rangle , \quad (6.22)$$

$$P_R[t(z_1, z_2)] \equiv \langle \theta(z_c^{(0)} - z^{(0)}) \delta[t(z_1, z_2) - t(z^{(0)}; z_1, z_2)] \rangle / \langle \theta(z_c^{(0)} - z^{(0)}) \rangle , \quad (6.23)$$

respectively. Often, a very significant contribution to the reflection probability comes from trajectories that do not enter the region  $z_1 \leq z \leq z_2$  of interest and it

is convenient to split off their contribution to  $P_R[t(z_1, z_2)]$  by writing

$$P_R[t(z_1, z_2)] \equiv P_R^{(0)} \delta[t(z_1, z_2)] + P_R^>[t(z_1, z_2)] . \quad (6.24)$$

The mean transmission and reflection times are obviously given by

$$\tau_T(z_1, z_2) = \int_0^\infty dt t P_T(t) , \quad \tau_R(z_1, z_2) = \int_0^\infty dt t P_R^>(t) . \quad (6.25)$$

## 6.4 Application to Simple Systems

### 6.4.1 Some Numerical Details

For static barriers the transmission probability for a finite wave packet is given by

$$|T|^2 = \int_0^\infty \frac{dk}{2\pi} |\phi(k)|^2 |T(k)|^2 \quad (6.26)$$

where  $|T(k)|^2$  is the stationary-state transmission probability for the ‘incident’ plane wave  $\exp(ikz)$  of wave number  $k$  and  $\phi(k)$  is the Fourier transform of the initial wave function  $\psi(z, 0)$ . Hence  $|T|^2$  and  $z_c^{(0)}$  can be calculated prior to solving the TDSE.

In the following subsections, the numerical method used to solve the TDSE is the fourth order (in time step  $\Delta t$ ) symmetrized product formula method developed by *De Raedt* [6.47]. For reasonable wave packet and barrier parameters, the resulting transmission probability

$$|T|^2 = \int_d^\infty dz |\psi(z, t_\infty)|^2 \quad (6.27)$$

converges very satisfactorily with decreasing  $\Delta t$  to the exact value, given by (6.26) for static barriers. Although the accuracy of the calculated trajectories is only of order  $\Delta t$ , that of the averaged quantities (6.20–23) is much better due to significant cancellation of errors between the numerators and denominators of the defining equations. Moreover, if one is interested in only  $\tau_T$  and  $\tau_R$ , the fact that Bohm trajectories do not intersect enables one to bypass the calculation of trajectories entirely. The alternative expressions, obtained from (6.17), are

$$\tau_T(z_1, z_2) = \frac{1}{|T|^2} \int_0^\infty dt \int_{z_1}^{z_2} dz |\psi(z, t)|^2 \theta[z - z_c(t)] , \quad (6.28)$$

$$\tau_R(z_1, z_2) = \frac{1}{|R|^2} \int_0^\infty dt \int_{z_1}^{z_2} dz |\psi(z, t)|^2 \theta[z_c(t) - z] , \quad (6.29)$$

where  $z_c(t)$ , the transmission–reflection bifurcation curve, is given by

$$\int_{z_c(t)}^{\infty} dz |\psi(z, t)|^2 = |T|^2 . \quad (6.30)$$

In most of the following applications of the Bohm trajectory approach to scattering problems the initial wave function is taken to be a Gaussian, i.e.

$$\psi(z, t = 0) = \frac{1}{[2\pi(\Delta z)^2]^{1/4}} \exp \left[ -\left( \frac{z - z_0}{2\Delta z} \right)^2 + ik_0 z \right] . \quad (6.31)$$

The width  $\Delta z$  of this minimum-uncertainty-product wave function is related to the width  $\Delta k$  of its Fourier transform  $\phi(k)$  by  $\Delta z \Delta k = 1/2$ ;  $z_0$  is the centroid of  $|\psi(z, 0)|^2$  and  $k_0$  is the centroid of  $|\phi(k)|^2 = [8\pi(\Delta z)^2]^{1/2} \exp[-(k - k_0)^2/(2\Delta k)^2]$ . The average energy of the initial wave packet is  $\bar{E} = [1 + (\Delta k/k_0)^2] E_0$  where  $E_0 \equiv \hbar^2 k_0^2 / 2m$  is the energy associated with wave number  $k_0$ . The prescription discussed above for selecting  $z_0$  takes the explicit form  $z_0 = -N^{-1}(1 - 10^{-4}|T|^2)\Delta z$  and the special starting position is given by  $z_c^{(0)} = z_0 + N^{-1}(1 - |T|^2)\Delta z$  where  $N^{-1}(x)$  is the inverse of the normal distribution function.

#### 6.4.2 Reflection Times for an Infinite Barrier

As a simple application [6.40] of the Bohm trajectory approach the mean reflection time is calculated for a region in front of the perfectly reflecting barrier  $V(z) = V_0 \theta(z)$  with  $V_0 \rightarrow \infty$ . For this special case reflection and dwell times are, of course, equivalent.

It is a straightforward exercise to show that the solution of the TDSE is

$$\begin{aligned} \psi(z, t) &= \alpha \exp[\beta_0 + \beta_2 z^2 + i(\gamma_0 + \gamma_2 z^2)] \\ &\times [\exp(\delta z + ie z) - \exp(-\delta z - ie z)] \theta(-z) \end{aligned} \quad (6.32)$$

where

$$\begin{aligned} \alpha &\equiv [2(\Delta z)^2 \eta/\pi]^{1/4} \exp\{-(\Delta z)^2 k_0^2 - (i/2) \arctan[\hbar t/2m(\Delta z)^2]\} , \\ \beta_0 &\equiv \eta(\Delta z)^2 [4(\Delta z)^4 k_0^2 - z_0^2 - 2k_0 z_0 \hbar t/m] , \\ \beta_2 &\equiv -\eta(\Delta z)^2 , \\ \gamma_0 &\equiv -\eta[4(\Delta z)^4 k_0 z_0 + 2(\Delta z)^4 k_0^2 \hbar t/m - z_0^2 \hbar t/2m] , \\ \gamma_2 &\equiv \eta(\hbar t/2m) , \\ \delta &\equiv 2\eta(\Delta z)^2 (z_0 + k_0 \hbar t/m) , \\ \varepsilon &\equiv \eta[4(\Delta z)^4 k_0 - z_0 \hbar t/m] , \\ \eta &\equiv [4(\Delta z)^4 + (\hbar t/m)^2]^{-1} . \end{aligned} \quad (6.33)$$

It should be noted that  $\psi(z, t)$  has a string of nodes at the points  $z_n \equiv -n\pi/k_0$  ( $n = 1, 2, \dots$ ) at the instant  $t = t_0 \equiv |z_0|/(\hbar k_0/m)$ .

After casting  $\psi(z, t)$  into the form  $R(z, t) \exp[iS(z, t)/\hbar]$  it is easy to obtain the following expressions for the quantum potential and particle velocity:

$$\begin{aligned} Q(z, t) &= \frac{\hbar^2}{2m} \left\{ -2\beta_2 \left[ 1 + 2\beta_2 z^2 + 2 \left( \frac{\delta \sinh 2\delta z + \varepsilon \sin 2\varepsilon z}{\cosh 2\delta z - \cos 2\varepsilon z} \right) z \right] \right. \\ &\quad \left. - 2 \frac{(\delta^2 \cosh 2\delta z + \varepsilon^2 \cos 2\varepsilon z)}{\cosh 2\delta z - \cos 2\varepsilon z} + \frac{(\delta \sinh 2\delta z + \varepsilon \sin 2\varepsilon z)^2}{(\cosh 2\delta z - \cos 2\varepsilon z)^2} \right\}, \end{aligned} \quad (6.34)$$

$$v(z, t) = \frac{\hbar}{m} \left[ 2\gamma_2 z + \left( \frac{\varepsilon \tanh \delta z - \delta \sin \varepsilon z \cos \varepsilon z \operatorname{sech}^2 \delta z}{\sin^2 \varepsilon z + \tanh^2 \delta z \cos^2 \varepsilon z} \right) \right]. \quad (6.35)$$

Numerical integration of  $v(z, t) = dz(t)/dt$  subject to the initial condition  $z(t = 0) = z^{(0)}$  yields the particle trajectory  $z(z^{(0)}, t)$ . A selection of such trajectories is shown in Fig. 6.1. The bending of the trajectories away from the nodes that appear at the instant  $t = t_0$  at the points  $z_n$  is quite striking, as is the bunching of trajectories just in front of the infinite barrier. Since  $v(z, t_0) < 0$  all the trajectories must turn around before  $t = t_0$ . For each particle trajectory  $z(z^{(0)}, t)$  it is easy to calculate numerically the time  $t(z^{(0)}; a, 0)$  spent by the particle in the region  $a \leq z \leq 0$ . The corresponding mean reflection time  $\tau_R(a, 0) = \langle t(z^{(0)}; a, 0) \rangle$  for the ensemble of particles described initially by  $\psi(z^{(0)}, 0)$  is obtained by integrating  $|\psi(z^{(0)}, 0)|^2 t(z^{(0)}; a, 0)$  over all  $z^{(0)}$ . Results for  $\tau_R(a, 0)$  are compared in Fig. 6.2 with the plane-wave ( $\Delta k = 0$ ) dwell time [6.21]

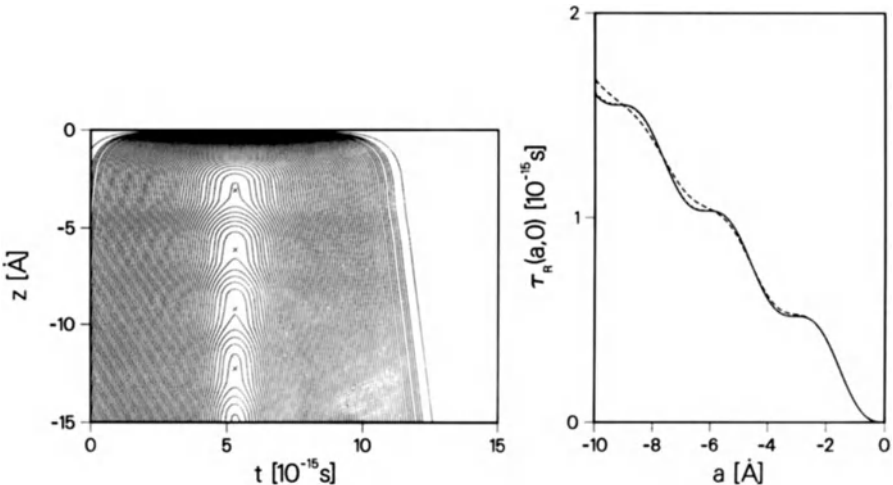
$$\tau_D(k_0; a, 0) = \tau_R(k_0; a, 0) = \frac{2|a|}{(\hbar k_0/m)} \left( 1 - \frac{\sin 2k_0 a}{2k_0 a} \right). \quad (6.36)$$

While  $\tau_R(a, 0)$  for  $\Delta k = 0.08 \text{ \AA}^{-1}$  shows significant departures from (6.36) for  $a \lesssim -2 \text{ \AA}$  the result for  $\Delta k = 0.02 \text{ \AA}^{-1}$  is barely distinguishable from (6.36) over the entire  $10 \text{ \AA}$  range shown in the figure. In this simple case the  $\Delta k = 0$  limit is numerically accessible via the Bohm trajectory technique.

#### 6.4.3 Transmission and Reflection Times for Rectangular Barriers

As an application of the trajectory approach involving tunneling [6.41], consider an electron with the initial Gaussian wave function (6.31) incident on the rectangular barrier  $V(z) = V_0 \theta(z) \theta(d - z)$  of height  $V_0 = 10 \text{ eV}$  and width  $d$ .

Figure 6.3 shows a selection of trajectories for  $\Delta k = 0.04$  and  $0.08 \text{ \AA}^{-1}$  with starting points  $z^{(0)}$  in the vicinity of the transmission–reflection bifurcation point  $z_c^{(0)}$ . The energy  $E_0$  of the incident wave packet is half of the barrier height  $V_0$ . The most striking difference between the two sets of trajectories is the factor of  $\sim 2$  difference in time scales for motion *within* the barrier.



▲

**Fig. 6.1.** Bohm trajectories  $z(z^{(0)}, t)$  for an initial Gaussian wave packet incident on the infinite potential barrier  $V(z) = V_0\theta(z)$  with  $V_0 \rightarrow \infty$ . The wave packet parameters are  $E_0 = 4$  eV,  $\Delta k = 0.04 \text{ \AA}^{-1}$  (i.e.,  $\Delta z = 12.50 \text{ \AA}$ ), and  $z_0 = -63 \text{ \AA}$ . The space-time points  $(z_n, t_0)$  at which  $\psi(z, t)$  is zero are indicated for  $n = 1, 2, 3$  and  $4$

**Fig. 6.2.** The average reflection time  $\tau_R(a, 0)$  for the region  $a \leq z \leq 0$  in front of the infinite barrier  $V(z) = V_0\theta(z)$  with  $V_0 \rightarrow \infty$ . The initial Gaussian wave packets have  $E_0 = 4$  eV and  $\Delta k = 0.08$  (dashed line) and  $0.02 \text{ \AA}^{-1}$  (dotted line). The plane-wave dwell time  $\tau_D(k_0; a, 0)$  is included for comparison (solid line)

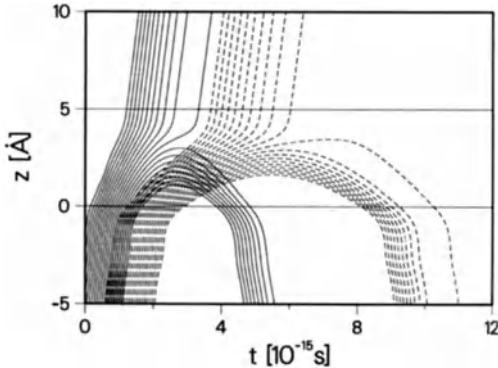


**Fig. 6.3.** Bohm trajectories for an initial Gaussian wave packet incident on a rectangular barrier of height  $V_0 = 10$  eV and width  $d = 5 \text{ \AA}$ . The location of the barrier is indicated by horizontal lines. The wave packet parameters are:  $E_0 = 5$  eV,  $\Delta k = 0.04 \text{ \AA}^{-1}$ ,  $z_0 = -71.80 \text{ \AA}$  (dashed lines);  $\Delta k = 0.08 \text{ \AA}^{-1}$ ,  $z_0 = -35.58 \text{ \AA}$  (solid lines)

Figure 6.4 shows the dependence of  $\tau_T(0, d)$ , calculated using the Bohm trajectory and Larmor clock<sup>4</sup> approaches, on the width  $d$  of the barrier for wave packets with  $E_0 = V_0/2$  and  $\Delta k = 0.04, 0.08$  and  $0.16 \text{ \AA}^{-1}$ . As  $d$  approaches zero both sets of calculations merge with the free-particle ( $V_0 = 0$ ) result

<sup>4</sup> For finite wavepackets, the Larmor clock results are obtained by averaging  $|\tau_T^{\text{SB}}(k; 0, d)|$  over  $k$  with weight factor  $|\phi(k)|^2 |T(k)|^2 / (2\pi |T|^2)$ .

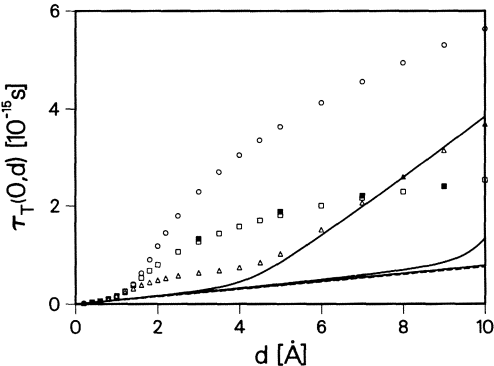


**Fig. 6.4.** Dependence of  $\tau_T(0, d)$  on  $d$  for a rectangular barrier of height  $V_0 = 10$  eV and incident energy  $E_0 = 5$  eV. The Bohm trajectory results are shown by circles for  $\Delta k = 0.04 \text{ \AA}^{-1}$ , squares for  $\Delta k = 0.08 \text{ \AA}^{-1}$  and triangles for  $\Delta k = 0.16 \text{ \AA}^{-1}$  and the corresponding  $k$ -averaged Larmor clock results by the lower, middle and upper solid curves, respectively. For  $\Delta k = 0.08 \text{ \AA}^{-1}$  and  $d = 3, 5, 7$  and  $9 \text{ \AA}$  the trajectory results recalculated using the value of  $z_0$  appropriate to  $\Delta k = 0.04 \text{ \AA}^{-1}$  are shown (filled squares). The free particle result  $d/(\hbar k_0/m)$  is indicated by the dashed line

$\tau_T^{\text{free}}(k_0; 0, d) = d/(\hbar k_0/m)$ . The Larmor clock results for  $\Delta k = 0.08 \text{ \AA}^{-1}$  are influenced by significant above-barrier transmission for  $d \geq 6 \text{ \AA}$  and  $\tau_T$  departs significantly from the  $\Delta k = 0.04 \text{ \AA}^{-1}$  results. For  $\Delta k = 0.16 \text{ \AA}^{-1}$  this effect is much more dramatic, setting in at  $d \sim 3 \text{ \AA}$ . The behaviour of the mean Bohm trajectory transmission time begins to change qualitatively when  $d$  becomes comparable to the characteristic tunneling length  $\kappa_0^{-1} = \hbar/[2m(V_0 - E_0)]^{1/2} \sim 0.9 \text{ \AA}$ , becoming strongly dependent on  $\Delta k$ . For  $\Delta k = 0.16 \text{ \AA}^{-1}$  the calculated transmission probability for  $d \geq 6 \text{ \AA}$  has a relatively large above-barrier resonant ( $|T(k)|^2 \sim 1$ ) contribution and is virtually independent of  $d$ ; in this region the Larmor clock and Bohm trajectory results are, not surprisingly, in good agreement.

The prescription discussed above for guaranteeing a well-defined transmission probability  $|T|^2$  requires that the centroid  $z_0$  of the initial Gaussian wave packet moves further from the barrier as  $\Delta z$  increases. For  $d = 3, 5, 7$  and  $9 \text{ \AA}$  the  $\Delta k = 0.08 \text{ \AA}^{-1}$  trajectory results recalculated with  $z_0$  values appropriate to  $\Delta k = 0.04 \text{ \AA}^{-1}$  are also shown in Fig. 6.4. Clearly only a small fraction of the large difference between the  $\Delta k = 0.04$  and  $0.08 \text{ \AA}^{-1}$  curves arises from the dependence on  $z_0$ . However, the calculated small changes in  $\tau_T$  with  $z_0$  are numerically significant and the mean transmission time does depend on  $z_0$  even though  $|T|^2$  does not. Since  $|\phi(k)|^2$  is independent of  $z_0$  for the initial Gaussian wave packet this means that, within the Bohm trajectory approach,  $\tau_T(0, d)$  cannot be obtained by integrating  $\tau_T(k; 0, d)|\phi(k)|^2 |T(k)|^2/(2\pi|T|^2)$  over  $k$  because the latter quantity is independent of  $z_0$ .

In Fig. 6.5 the dependence of  $\tau_T(0, d)$  on  $E_0$  and  $\Delta k$  is shown for a relatively narrow ( $d = 3 \text{ \AA}$ ) barrier in order to suppress possible above-barrier resonance effects. The Larmor clock and Bohm trajectory results are qualitatively different in both their dependence on  $E_0$  and  $\Delta k$  until  $E_0$  is well above the barrier height  $V_0$ . In Fig. 6.6 the same comparison is made for a wider ( $d = 5 \text{ \AA}$ ) barrier and an incident wave packet with a relatively small energy width ( $\Delta k = 0.02 \text{ \AA}^{-1}$ ) in order to highlight any resonance effects. The Larmor clock result for  $\tau_T(0, d)$

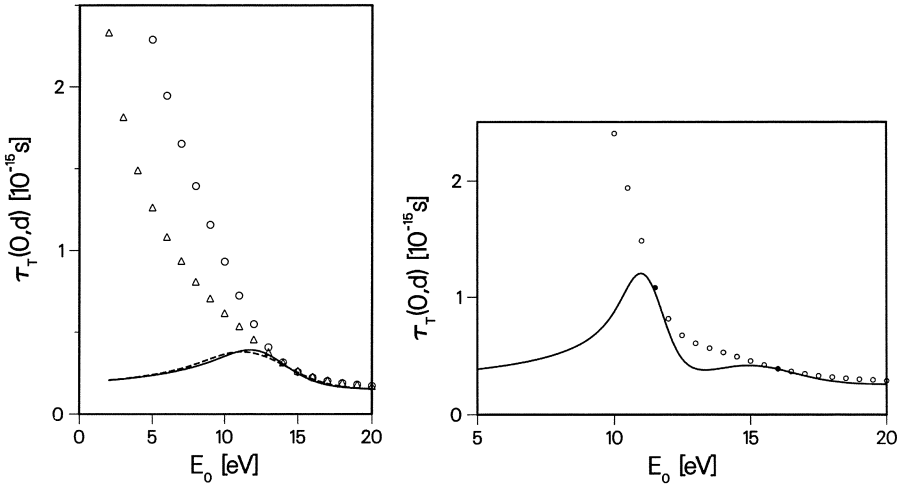


**Fig. 6.5.** Dependence of  $\tau_T(0,d)$  on the energy  $E_0$  of a Gaussian wave packet incident on a rectangular barrier of height  $V_0 = 10 \text{ eV}$  and width  $d = 3 \text{ \AA}$ . The Bohm trajectory results are shown by circles for  $\Delta k = 0.04 \text{ \AA}^{-1}$  and triangles for  $\Delta k = 0.08 \text{ \AA}^{-1}$  and the corresponding Larmor clock results by the solid and dashed lines, respectively. The first above barrier resonance  $E_r^{(1)}$  at  $14.175 \text{ eV}$  is the only one below  $20 \text{ eV}$

**Fig. 6.6.** Dependence of  $\tau_T(0,d)$  on the energy  $E_0$  of an initial Gaussian wave packet with  $\Delta k = 0.02 \text{ \AA}^{-1}$  incident on a rectangular barrier of height  $V_0 = 10 \text{ eV}$  and width  $d = 5 \text{ \AA}$ . The Larmor clock results are shown by the solid curve and the trajectory results by circles (those for the above-barrier resonances at  $E_r^{(1)} = 11.503 \text{ eV}$  and  $E_r^{(2)} = 16.012 \text{ eV}$  by filled circles)

shows considerable structure, peaking fairly close to the above-barrier resonances at  $E_r^{(1)}$  and  $E_r^{(2)}$ . The trajectory result, on the other hand, decreases monotonically exhibiting no apparent resonant structure; however, the contribution to the mean dwell time from transmitted particles, i.e.  $|T|^2 \tau_T(0,d)$ , does have well-defined resonance peaks. As expected, the agreement between the Bohm trajectory and Larmor clock results is best very close to the resonances where  $|T|^2 \sim 1$ .

Bohm trajectory transmission time distributions  $P_T[t(0,d)]$  are shown in histogram form in Fig. 6.7 for barrier widths close to ( $d = 2.0 \text{ \AA}$ ) and well above ( $d = 5.0 \text{ \AA}$ ) the transparent to opaque barrier ‘crossover’ evident in Fig. 6.4. For each case there is a well-defined minimum and most probable transmission time. However, each distribution has a long tail on the high side of the peak arising from transmitted trajectories very close to the transmission–reflection bifurcation where the time spent inside the barrier diverges. Transmission times very much in excess of the average, although rare, are possible and could have implications for submicron single-electron devices based on tunneling.

Figure 6.8 shows the reflection time distributions  $P_R[t(0,d)] = P_R^0 \delta[t(0,d)] + P_R^>[t(0,d)]$  corresponding to the ( $d = 5 \text{ \AA}$ ) transmission time distributions  $P_T[t(0,d)]$  in the bottom panel of Fig. 6.7. The component

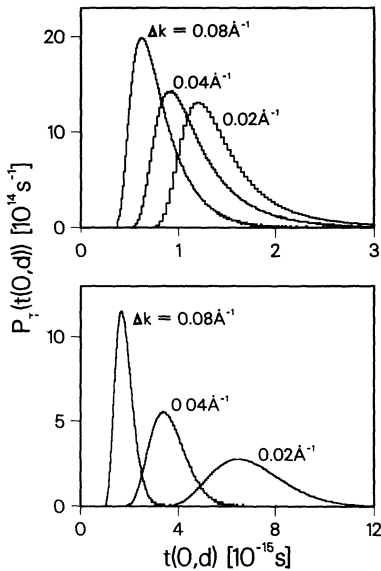


**Fig. 6.7.** Transmission time distributions  $P_T[t(0,d)]$  calculated using the Bohm trajectory approach for a barrier of height  $V_0 = 10$  eV and width  $d$  of  $2.0 \text{ \AA}$  (top) and  $5.0 \text{ \AA}$  (bottom). In all cases the incident energy  $E_0 = 5$  eV

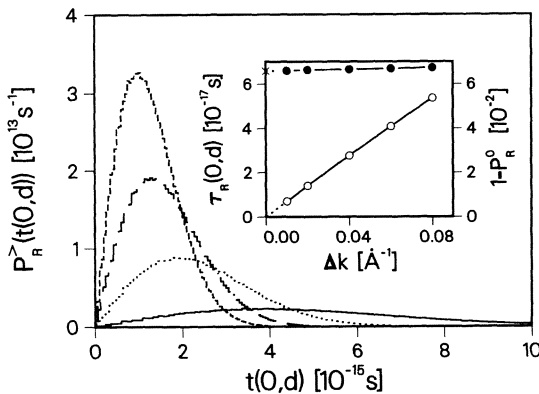


**Fig. 6.8.** Reflection time distributions  $P_R^>[t(0,d)]$  for a rectangular barrier of height  $V_0 = 10$  eV and width  $d = 5 \text{ \AA}$ . The wave packet parameters are  $E_0 = 5$  eV and  $\Delta k = 0.02$  (solid line),  $0.04$  (dotted line),  $0.06$  (chained line) and  $0.08 \text{ \AA}^{-1}$  (dashed line).  $P_R^>[t(0,d)]$  is normalized to  $(1 - P_R^0)$  which is shown in the inset along with the mean reflection time  $\tau_R(0,d)$  as open and filled circles, respectively. The plane-wave dwell time  $\tau_D(k_0; 0, d)$  is indicated by X. The solid and dotted lines in the inset are guides to the eye

$P_R^>[t(0,d)]$  for electrons which actually enter the barrier region before being reflected is normalized to  $(1 - P_R^0)$  which is shown in the inset along with  $\tau_R(0,d)$  as a function of  $\Delta k$ . Over the range  $0.01 \text{ \AA}^{-1} \leq \Delta k \leq 0.08 \text{ \AA}^{-1}$  at least, as  $\Delta k$  decreases towards the plane-wave limit ( $\Delta k = 0$ ) a smaller and smaller fraction  $(1 - P_R^0)$  of the reflected electrons spends longer and longer in the barrier region in such a way that the mean reflection time  $\tau_R(0,d)$  has relatively little depend-

ence on  $\Delta k$ . It is tempting to extrapolate the calculated results for  $\tau_R(0, d)$  to  $\Delta k = 0$  in order to obtain  $\tau_R(k_0; 0, d)$  which, at least for this particular case, would be very close to the plane-wave dwell time  $\tau_D(k_0; 0, d)$  given by (6.5), as shown in the figure. However, if the stationary-state Bohm trajectory result,  $\tau_T(k_0; 0, d) = |T(k_0)|^{-2} \tau_D(k_0; 0, d)$ , of Spiller et al. [6.48] is correct then  $\tau_R(k_0; 0, d)$  must be zero (for  $|R(k_0)|^2 \neq 0$ ) because  $|T(k_0)|^2 \tau_T(k_0; 0, d) = \tau_D(k_0; 0, d)$  exhausts the sum rule (6.1). Unfortunately, it would be necessary to extend the time-dependent wave packet calculations of  $\tau_R(0, d)$  to much smaller values of  $\Delta k$  in order to decide whether it remains finite or eventually plummets to zero in the plane-wave limit. We believe that the former alternative is more likely to be correct because it is not obvious that one can determine the temporal characteristics of a scattering process with  $0 < |T|^2 < 1$  by studying only the stationary-state ( $\Delta k = 0$ ) case. For example, Spiller et al. use the time-independent particle velocity  $v(z) = (1/m)\partial S(z)/\partial z$  which is positive for all  $z$  and apparently assume that it is a property of transmitted electrons only rather than an average over transmitted and reflected electrons. Hence, all their calculated trajectories are transmitted ones, *even if*  $|T(k_0)|^2 \ll 1$ . We believe that for  $|T|^2 < 1$  the plane-wave limit should be approached using time-dependent calculations with initial wave packets of greater and greater spatial extent, as in Sect. 6.4.2. Unfortunately, it is clear that calculations for initial wave packets with much smaller  $\Delta k$  than those considered in Figs. 6.4, 8 will be required to obtain the plane-wave limit of  $\tau_T(0, d)$  and  $\tau_R(0, d)$  for finite opaque barriers. This is expected to be computationally demanding.

An interesting question [6.7, 25] is “What is the average time  $\tau_R(z_1, z_2)$  spent in a region  $z_1 \leq z \leq z_2$  on the far side ( $z_1 > d$ ) of a rectangular barrier by electrons that are ultimately *reflected*?”. Although the potential  $V(z)$  is zero for  $z > d$  and there is apparently nothing to scatter an electron back through the barrier the Larmor clock approach leads to a non-zero result for  $\tau_R(z_1 > d, z_2)$ . On the other hand, although the quantum potential  $Q(z, t)$  for  $z > d$  could conceivably launch an electron back through the barrier this has never happened in any of our calculations using the trajectory approach and hence  $\tau_R(z_1 > d, z_2)$  appears to be zero.

#### 6.4.4 Coherent Two-Component Incident Wave Packet

The non-intersecting property of Bohm trajectories is graphically illustrated by the scattering of an initial incident wave packet which is the *coherent* sum of two widely separated but otherwise identical Gaussians, i.e.

$$\psi_\gamma(z, t=0) = \frac{\left[ \exp\left(\frac{-(z-z_0)^2}{4(\Delta z)^2}\right) + \exp\left(\frac{-(z-z_0+\gamma\Delta z)^2}{4(\Delta z)^2}\right) \right] \exp(ik_0 z)}{2^{1/2} \left[ 1 + \exp\left(-\frac{\gamma^2}{8}\right) \right]^{1/2} [2\pi(\Delta z)^2]^{1/4}}, \quad (6.37)$$

with  $\gamma$  very much greater than 1 (the centroid of the second Gaussian is located  $\gamma\Delta z$  further from the barrier than the centroid  $z_0$  of the first). It readily follows from (6.26) that the transmission probability is given by

$$|T_\gamma|^2 = \frac{1}{1 + \exp(-\gamma^2/8)} \int_0^{+\infty} \frac{dk}{2\pi} [1 + \cos \gamma(k - k_0)\Delta z] |\phi_{\gamma=0}(k)|^2 |T(k)|^2 \quad (6.38)$$

where  $\phi_{\gamma=0}(k)$  is the Fourier transform of a single (normalized) Gaussian wave function of width  $\Delta z$  and  $|T(k)|^2$  is the corresponding plane-wave transmission probability. Using the fact that  $|T_{\gamma=\infty}|^2 = |T_{\gamma=0}|^2$  we restrict our attention to the case  $\gamma \gg 1$  and for definiteness consider an opaque barrier so that the transmission-reflection bifurcation point  $z_{c,\gamma}^{(0)}$  is to the right of  $z_0$ . Now, for  $z \geq z_0$  and  $t$  sufficiently small that there is still negligible overlap of the two components of the wave packet,  $|\psi_\gamma(z, t)|^2$  is equal to  $(1/2)|\psi_{\gamma=0}(z, t)|^2$  and  $Q_\gamma(z, t)$  is equal to  $Q_{\gamma=0}(z, t)$  to a very good approximation (recall that the quantum potential  $Q$  depends only on the form of  $|\psi|^2$  so that the factor of 1/2 is irrelevant). This means that, for sufficiently large  $\gamma$ , electrons with starting points  $z^{(0)}$  to the right of but not too close to the bifurcation point  $z_{c,\gamma=0}^{(0)}$  of the single Gaussian wave packet are transmitted following trajectories very similar to those for the single Gaussian case, as can be seen in Fig. 6.9. However, it is clear from the defining equation, (6.19), that  $z_{c,\gamma}^{(0)}$  must be further from the barrier than  $z_{c,\gamma=0}^{(0)}$  because  $|\psi_\gamma(z, 0)|^2$  is smaller than  $|\psi_{\gamma=0}(z, 0)|^2$  by a factor of 2 for  $z \gtrsim z_0$ . Hence, some of the trajectories that were initially reflected by the barrier, namely

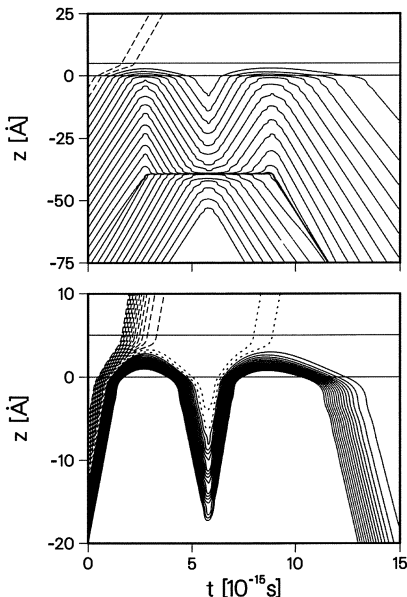


**Fig. 6.9.** Two selections of Bohm trajectories  $z(z^{(0)}, t)$  for an initial wave packet which is the coherent sum of two widely separated but otherwise identical Gaussians incident on a rectangular barrier ( $V_0 = 10$  eV,  $d = 5$  Å,  $E_0 = 5$  eV and  $\Delta k = 0.08$  Å<sup>-1</sup>). There are two distinct types of transmitted trajectories: those that are transmitted directly (long-dashed lines) and those that are transmitted after first being reflected by the barrier (short-dashed lines)

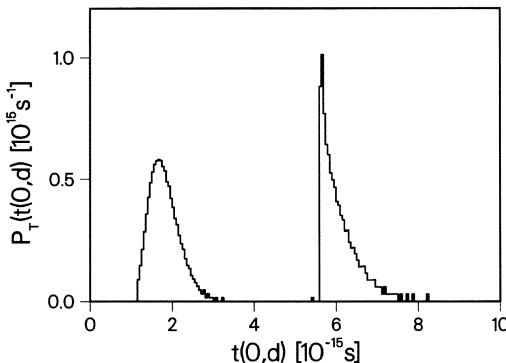


**Fig. 6.10.** The distribution  $P_T[t(0,d)]$  of transmission times  $t(0,d)$  for a double-Gaussian wave packet incident on a rectangular barrier. The wave packet and barrier parameters are those of Fig. 6.9

those with  $z_{c,\gamma}^{(0)} \leq z^{(0)} \leq z_{c,\gamma=0}^{(0)}$ , must ultimately be transmitted. What happens, of course, is that eventually the (initially) reflected part of the first component of the wave packet significantly overlaps and interferes with the incoming second component. The resulting strong fluctuations in the quantum potential launch the initially ‘unsuccessful’ trajectories back towards the barrier for another ‘attempt’. Those with  $z^{(0)} \geq z_{c,\gamma}^{(0)}$  are transmitted this time (see the bottom panel of Fig. 6.9).

The Bohm trajectories of Fig. 6.9 are for the initial wave packet  $\psi_\gamma(z, t = 0)$  with  $E_0 = 5$  eV,  $z_0 = -35.6$  Å,  $\Delta z = 6.25$  Å ( $\Delta k = 0.08$  Å $^{-1}$ ) and  $\gamma = 13$  incident on the rectangular barrier  $V(z) = V_0 \theta(z) \theta(d - z)$  with  $V_0 = 10$  eV and  $d = 5$  Å. The prominent feature in the middle of the top panel arises when the two trajectories originating at the centroids of the two Gaussian components of the initial wave packet come within about 10 Å of each other during the collision of the reflected component with the incoming component of  $\psi_\gamma(z, t)$ , sandwiching all of the trajectories with  $z_0 - \gamma\Delta z < z^{(0)} < z_0$  between them. It is clear from the bottom panel of the figure that, on average, those trajectories that are transmitted without being initially reflected involve considerably shorter transmission times than those which are initially reflected. This is apparent in the calculated transmission time distribution shown in Fig. 6.10. Clearly, using the fact that Bohm trajectories do not intersect can allow one to predict important qualitative features of both trajectory maps and transmission time distributions.

#### 6.4.5 Transmission Times for Time-Modulated Barriers

The time-modulated barrier approach of Büttiker and Landauer [6.26, 27] was motivated by the belief that adding a small oscillatory component  $V_1 \cos \omega t$  to a static barrier leads to distinct low ( $\omega \ll \tau_T^{-1}$ ) and high ( $\omega \gg \tau_T^{-1}$ ) frequency regimes in the resulting tunneling behaviour ( $\tau_T$  is the mean transmission time for the unperturbed static barrier). In particular, it is argued that for  $\omega \ll \tau_T^{-1}$  the tunneling electron ‘sees’ a static barrier to a very good approximation while for  $\omega \gg \tau_T^{-1}$  it ‘sees’ the time-averaged barrier but, in addition, now has a significant

probability of absorbing or emitting modulation quanta leading to transmission and reflection side-bands. In their analysis of this appealing physical picture Büttiker and Landauer considered a plane wave  $\exp(ikz)$  of energy  $E = \hbar^2 k^2 / 2m$  ‘incident’ on the time-modulated rectangular barrier  $V(z, t) = (V_0 + V_1 \cos \omega t) \theta(z) \theta(d - z)$  with  $V_1 \ll \hbar\omega \ll E, V_0 - E$ . In the low frequency limit they showed that the probability of transmission at the first-order side-band energies  $E \pm \hbar\omega$  is given by

$$|T_{\pm}|^2 = [V_1 \tau_T^{BL}(k)/2\hbar]^2 |T(k)|^2 \quad (\omega \rightarrow 0) \quad (6.39)$$

where

$$\tau_T^{BL}(k) = (m/\hbar\kappa) |\partial \ln T(k)/\partial \kappa| \quad (\kappa = [2m(V_0 - E)/\hbar^2]^{1/2}) \quad (6.40)$$

is the well-known Büttiker–Landauer traversal time for a rectangular barrier. Støvneng and Hauge [6.49] and also Jauho and Jonson [6.50] showed that (6.39) holds for an arbitrary barrier when (6.40) is replaced by

$$\tau_T^{BL}(k) = \hbar |\partial \ln T(k)/\partial \bar{V}| \quad (6.41)$$

where  $\bar{V}$  is the average height of the barrier. However, both groups expressed reservations about the identification of  $\tau_T^{BL}(k)$  with the actual traversal time. It should be recalled that (6.41) is identical to the modulus of the mean transmission time of Sokolovski and Baskin,  $|\tau_T^{SB}(k)|$ .

Recently De Raedt et al. [6.51] numerically studied the scattering of Gaussian wave packets by time-modulated rectangular barriers but were unable to extract  $\tau_T$  from the frequency dependence of the calculated transmission probability. Our calculations for a significantly different range of parameters [6.52] support this conclusion. Figure 6.11 shows the dependence of  $|T|^2$  on modulation frequency  $\omega$  for an opaque rectangular barrier. The modulation amplitude  $V_1$  is sufficiently small that only the first-order side-bands are important. The transmission probability is strongly enhanced when the upper side-band at  $E_0 + \hbar\omega$  coincides with the first ( $n = 1$ ) and second ( $n = 2$ ) above-barrier resonances of the unmodulated barrier at  $E_r^{(n)} = V_0 + (\hbar^2/2m)(n\pi/d)^2$ . The oscillatory structure at low frequencies is due to the finite spatial width  $\Delta z$  of the wave packet. The frequency range over which such oscillations are of non-negligible amplitude decreases with increasing  $\Delta z$  and is expected to shrink to zero in the plane-wave limit ( $\Delta z \rightarrow \infty$ ) leaving a smoothly varying featureless curve in the vicinity of  $\tau_T^{BL}(k_0)^{-1}$  ( $= 0.26 \times 10^{16} \text{ s}^{-1}$ ). This trend is confirmed by calculations with larger  $\Delta z$  than those shown. The figure shows  $|T|^2$  for both  $V_1 \sin \omega t$  and  $V_1 \cos \omega t$  modulations. We prefer the former because in the static limit  $\omega \rightarrow 0$  the (total) barrier height is then the original unmodulated barrier height  $V_0$  rather than  $V_0 + V_1$ . Only results for the  $V_1 \sin \omega t$  modulations are shown in the remaining figures of this subsection.

We now consider the time-modulated barrier from the Bohm trajectory point of view which clearly shows that there is no reason to expect a signature of

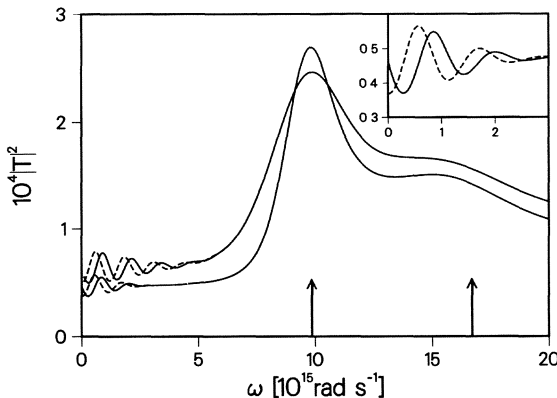


**Fig. 6.11.** The frequency dependence of the transmission probability  $|T|^2$  for a Gaussian wave packet incident on a time-modulated rectangular barrier of unmodulated height  $V_0 = 10$  eV and width  $d = 5$  Å. The results for the modulation  $V_1 \theta(z)\theta(d-z)\sin\omega t$  are shown by the solid curves and for  $V_1 \theta(z)\theta(d-z)\cos\omega t$  by the dashed curves with  $V_1 = V_0/50 = 0.2$  eV. The incident energy  $E_0 = 5$  eV,  $z_0 = -71.8$  Å and  $\Delta k = 0.08$  Å $^{-1}$  for the upper curves (near  $\omega = 0$ ) and  $\Delta k = 0.04$  Å $^{-1}$  for the lower curves. The resonance condition  $\hbar\omega = E_r^{(n)} - E_0$  for the first-order sideband is indicated by an arrow for  $n = 1$  and 2. The inset shows the low frequency behaviour for  $\Delta k = 0.04$  Å $^{-1}$

$\tau_T$  in the frequency dependence of  $|T|^2$ . In the limit  $t \rightarrow \infty$  when the scattering of the wave packet is complete each trajectory  $z(z^{(0)}, t)$ , with the exception of the one with  $z^{(0)} = z_c^{(0)}$ , can be labelled as either transmitted or reflected

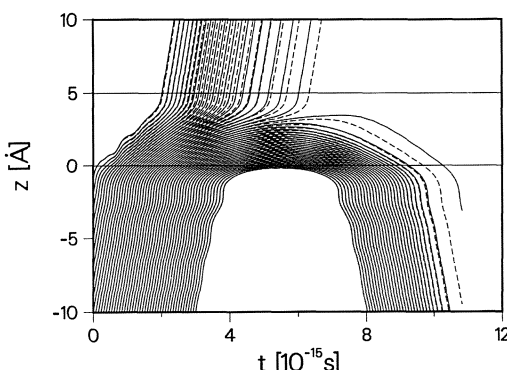
$$\theta_T(z^{(0)}) \equiv \theta(z^{(0)} - z_c^{(0)}) = \begin{cases} 1 & (\text{transmitted trajectory}) \\ 0 & (\text{reflected trajectory}) \end{cases}. \quad (6.42)$$

Now, for the trajectory starting at a particular  $z^{(0)}$ , transmission is ‘all or nothing’, i.e.  $\theta_T(z^{(0)}) = 1$  or 0. Hence, if the original barrier is perturbed in some way there are four distinct possibilities for the effect of the perturbation on  $\theta_T$ , only three of which can occur for a given perturbation because Bohm trajectories do not intersect. If the transmission probability  $|T|^2 = \langle \theta_T(z^{(0)}) \rangle$  increases then one possibility, denoted by the shorthand  $0 \rightarrow 1$ , is that the perturbation causes  $\theta_T(z^{(0)})$  to change from 0 to 1; for the two other possibilities,  $0 \rightarrow 0$  and  $1 \rightarrow 1$ ,  $\theta_T(z^{(0)})$  is unaffected by the perturbation. The important  $0 \rightarrow 1$  possibility occurs for and *only* for  $z_c^{(0)} \leq z^{(0)} \leq z_{c,0}^{(0)}$  where  $z_{c,0}^{(0)}$  denotes  $z_c^{(0)}$  for the unperturbed system. If  $|T|^2$  decreases because of the perturbation the three possibilities are  $1 \rightarrow 0$ ,  $0 \rightarrow 0$  and  $1 \rightarrow 1$ , the first occurring only for  $z_{c,0}^{(0)} \leq z^{(0)} \leq z_c^{(0)}$ . Any change in the transmission probability arises solely from those particle trajectories for which the perturbation changes  $\theta_T(z^{(0)})$ , namely from 0 to 1 if  $|T|^2$  increases or from 1 to 0 if  $|T|^2$  decreases. For example, if the relative change in  $|T|^2$  due to the perturbation is a very small decrease then the crucial  $1 \rightarrow 0$  trajectories have  $z^{(0)}$  very close to and to the right of  $z_{c,0}^{(0)}$ . The corresponding

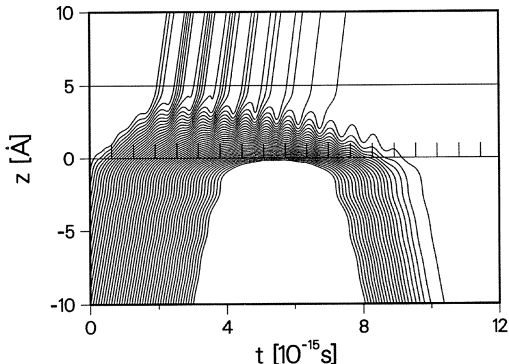
trajectories of the unperturbed system are characterized by anomalously long transmission times far out in the tail of the transmission time distribution (see the  $\omega = 0$  distribution in Fig. 6.14 below). Similarly, if the relative change in  $|T|^2$  is a very small increase then the trajectories of the unperturbed system that are most dramatically changed by the perturbation (i.e.  $0 \rightarrow 1$ ) are characterized by anomalously large *reflection* times. These can be especially atypical in this case particularly for an opaque barrier for which the typical reflected trajectory does not even reach the barrier and has a reflection time  $t(z^{(0)}; 0, d)$  of zero. Clearly, at least within the Bohm interpretation, there is no reason whatsoever to expect anything special to happen to  $|T|^2$  when the modulation frequency  $\omega$  passes through  $\tau_T^{-1}$ .

Figure 6.12 compares a selection of Bohm trajectories for an unmodulated rectangular barrier with the corresponding trajectories when a small modulation  $V_1 \sin \omega t$  is applied to the barrier with  $V_1$  and  $\hbar\omega$  satisfying the conditions  $V_1 \ll \hbar\omega \ll E_0$ ,  $V_0 - E_0$  of the Büttiker–Landauer papers. Although in this case the perturbation leads to a decrease in  $|T|^2$ , none of the pairs of trajectories shown here have  $z^{(0)}$  close enough to  $z_{c,0}^{(0)}$  to be of the  $1 \rightarrow 0$  type associated with the decrease, but the trend is clear. Increasing the density of trajectories would, of course, eventually reveal such trajectories.

Figure 6.13 shows a selection of trajectories for the special case in which the modulation frequency satisfies the resonance condition  $E_0 + \hbar\omega = E_r^{(1)}$  (we are ignoring the very small difference between  $E_0$  and  $\bar{E}$ ). Those trajectories that spend a significant length of time inside the barrier show well-defined oscillations of period  $2\pi/\omega$ . Since the classical force  $-\partial V(z, t)/\partial z$  is zero for  $0 < z < d$  these oscillations arise indirectly from the  $V_1 \sin \omega t$  modulation through the quantum force  $-\partial Q(z, t)/\partial z$ . Although most of the transmitted trajectories enter the barrier at fairly regular intervals they leave in bunches. This combined with the general increase in  $t(z^{(0)}; 0, d)$  as  $z^{(0)}$  approaches  $z_c^{(0)}$  leads to the multi-peaked transmission time distribution shown in Fig. 6.14 where it is compared with the distribution for a far-from-resonance modulation frequency and for the static case.



**Fig. 6.12.** Bohm trajectories for a Gaussian wave packet with  $E_0 = 5$  eV,  $\Delta k = 0.04 \text{ \AA}^{-1}$  and  $z_0 = -71.8 \text{ \AA}$  incident on the static barrier  $V_0 \theta(z) \theta(d - z)$  and on the time-modulated barrier  $(V_0 + V_1 \sin \omega t) \theta(z) \theta(d - z)$  are shown by the solid and dashed curves, respectively. The barrier parameters are  $V_0 = 10$  eV,  $d = 5 \text{ \AA}$ ,  $V_1 = 0.2$  eV and  $\hbar\omega = 1.0$  eV



**Fig. 6.13.** Bohm trajectories for a Gaussian wave packet with  $E_0 = 5$  eV,  $\Delta k = 0.04 \text{ \AA}^{-1}$  and  $z_0 = -71.8 \text{ \AA}$  incident on the time-modulated barrier  $(V_0 + V_1 \sin \omega t) \theta(z) \theta(d - z)$  with  $V_0 = 10$  eV,  $d = 5 \text{ \AA}$ ,  $V_1 = 0.2$  eV and  $\hbar\omega = E_r^{(1)} - E_0$ . The vertical lines along the time axis indicate integral multiples of the modulation period  $2\pi/\omega$

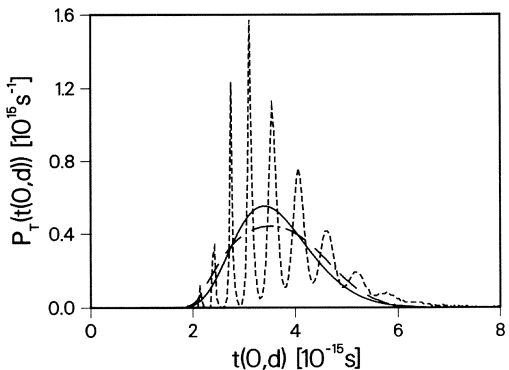


**Fig. 6.14.** Transmission time distributions  $P_T[t(0, d)]$  for  $\hbar\omega = 0$  (solid line),  $\hbar\omega = 1$  eV (chained line) and  $\hbar\omega = E_r^{(1)} - E_0$  (dashed line) for a Gaussian wave packet with  $E_0 = 5$  eV,  $\Delta k = 0.04 \text{ \AA}^{-1}$  and  $z_0 = -71.8 \text{ \AA}$  incident on the time-modulated barrier  $(V_0 + V_1 \sin \omega t) \theta(z) \theta(d - z)$  with  $V_0 = 10$  eV,  $d = 5 \text{ \AA}$  and  $V_1 = 0.2$  eV

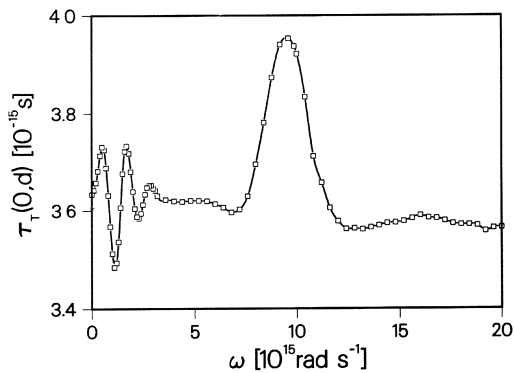


**Fig. 6.15.** The frequency dependence of the mean transmission time for the wave packet and barrier parameters of Fig. 6.14. The solid line is a guide to the eye

Figure 6.15 shows the dependence of the mean transmission time  $\tau_T(0, d)$  on modulation frequency  $\omega$  for one of the cases considered in Fig. 6.11. Although  $\tau_T(0, d)$  is significantly enhanced at the  $n = 1$  resonance it is considerably less sensitive to  $\omega$  than is  $|T|^2$ .

The distribution of energy for a wave packet is usually considered in terms of the free-particle energy  $E(k) \equiv \hbar^2 k^2 / 2m$ , i.e.

$$P(E, t) = (2\pi)^{-1} \int_{-\infty}^{+\infty} dk |\phi(k, t)|^2 \delta(E - E(k)) \quad (6.43)$$

where  $\phi(k, t)$  is the Fourier transform of  $\psi(z, t)$ . Now, in Bohm's interpretation an electron with position  $z$  at time  $t$  has a well-defined energy

$$E(z, t) = (m/2)v(z, t)^2 + V(z, t) + Q(z, t) . \quad (6.44)$$

Hence, an alternative way of distributing the energy of a wave packet is in terms of  $E(z, t)$ , i.e.

$$P^B(E, t) = \int_{-\infty}^{+\infty} dz |\psi(z, t)|^2 \delta(E - E(z, t)) \quad (6.45)$$

$$= \int_{-\infty}^{+\infty} dz^{(0)} |\psi(z^{(0)}, 0)|^2 \delta(E - E(z^{(0)}, t), t) . \quad (6.46)$$

Both distributions (6.43 and 6.46) lead to the same expectation value,  $\bar{E}(t)$ , for the energy [6.14].

In the standard interpretations of quantum mechanics one has no way of knowing where, on average, a transmitted electron associated with the upper side-band absorbed a modulation quantum of energy  $\hbar\omega$ . Despite this, it has been suggested [6.26] that for an opaque rectangular barrier the absorption occurs at the leading edge of the barrier because the tunneling electron then 'sees' an effective barrier that is lower by  $\hbar\omega$  for all of its journey through the classically forbidden region. This sounds very plausible. However, it seems inconsistent with the idea that it is only when the time spent by an electron inside the barrier is much greater than  $\omega^{-1}$  that there is a significant probability for the absorption of a modulation quantum [6.26]. This inconsistency arises at least partly from attempting to picture an electron in a state extending over all space as a localized particle during the tunneling process within an interpretation which does not allow such pictures.

In the Bohm interpretation, on the other hand, one can follow the energy distribution for the 'to be transmitted part' of the wave packet as a function of time, right from  $t = 0$ , simply by replacing the lower limit on the integral over  $z^{(0)}$  in (6.46) by  $z_c^{(0)}$ . Figure 6.16 shows the evolution of the particle energy  $E(z, t)$ , with  $t$  implicit, for a selection of Bohm trajectories  $z(z^{(0)}, t)$  calculated for the wave packet and barrier parameters of Fig. 6.13 where  $\hbar\omega = E_r^{(1)} - E_0$ . For this resonant situation the reflected trajectories shown all have  $E(z, t) \sim E_0$  and the transmitted ones  $E(z, t) \sim E_0 + \hbar\omega$  at sufficiently large  $t$ . It should be noted that the transmitted electrons associated with the upper side-band experience large fluctuations in energy that continue well beyond the barrier region before their energy finally settles down to  $E_0 + \hbar\omega$ .

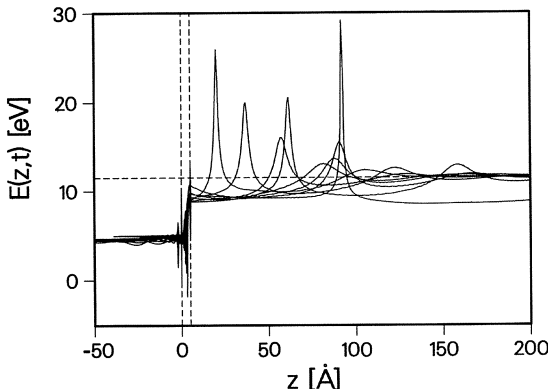


**Fig. 6.16.** The particle energy  $E(z, t)$  along a selection of Bohm trajectories  $z(z^{(0)}, t)$  with  $t$  implicit and  $-39.0 \text{ \AA} \leq z^{(0)} \leq -21.0 \text{ \AA}$  in steps of  $1 \text{ \AA}$  for the wave packet and barrier parameters of Fig. 6.13 ( $z_c^{(0)} = -28.54 \text{ \AA}$ ). The resonance energy  $E_r^{(1)}$  of the static rectangular barrier is indicated by the horizontal dashed line and the position of the barrier by the vertical dashed lines

#### 6.4.6 Transmission Times for Symmetric Double Rectangular Barriers

Larmor clock results [6.25] for  $\tau_T(k; 0, z)$  with  $0 \leq z \leq d$  have been calculated for a plane-wave electron of wave number  $k$  ‘incident’ on the symmetric double rectangular barrier  $V_0[\theta(z)\theta(a-z) + \theta(z-d+a)\theta(d-z)]$ . The detailed results for the special case of resonant transmission with  $|T(k=k_r)|^2 = 1$  are directly relevant to this chapter because the Larmor clock and Bohm trajectory approaches give identical results for the limiting cases of perfect transmission and perfect reflection.<sup>5</sup> Rather than simply reproduce these  $|T(k_r)|^2 = 1$  results we instead discuss how the Bohm trajectory approach illuminates an interesting puzzle connected with the Larmor clock approach.

For the special case  $|T(k_r)|^2 = 1$  the average ‘transmission speed’ defined in [6.25] as

$$\bar{v}_T(k; z) \equiv [\partial\tau_T(k; 0, z)/\partial z]^{-1} \quad (6.47)$$

is given by

$$\bar{v}_T(k_r; z) = j_{k_r}(z)/P_{k_r}(z) = (\hbar k_r/m)/|\psi_{k_r}(z)|^2 \quad (6.48)$$

where the plane-wave probability current density  $j_k(z) = \hbar k/m$  is independent of  $z$ . Now, a glance at (6.13) reveals that an alternative expression for the Bohm particle velocity is  $v(z, t) = j(z, t)/P(z, t)$ . This definition is preferable to the familiar  $v(z, t) \equiv m^{-1}\partial S(z, t)/\partial z$  because it is readily generalized [6.53] to particles described by the Pauli or Dirac equations simply by inserting the appropriate expressions for  $j$  and  $P$ . Clearly,  $\bar{v}_T(k_r; z)$  is identical to the plane-wave limit of  $v(z, t)$  for the special case  $|T(k=k_r)|^2 = 1$  considered here. This is not true in general, not even for resonant transmission with  $|T(k=k_r)|^2 < 1$  as is the case when the transmission probabilities for the individual barriers are unequal for  $k = k_r$ .

<sup>5</sup> Leavens and Aers were not familiar with Bohm’s trajectory interpretation when [6.25] was written.

For  $k = k_r^{(n)}$  with  $n > 1$  it is possible to have quasinodes of the probability density in the well region  $a \leq z \leq d - a$  where  $|\psi_k(z)|^2$  is so small that (6.48) leads to  $\bar{v}_T(z) \gg c$ , the speed of light. However, if the Schrödinger expressions for the plane-wave probability and probability current densities  $P_k(z)$  and  $j_k$  are replaced in (6.48) by the corresponding expressions [6.54] for positive energy spin-up (or down) Dirac electrons then one can readily prove [6.25] that  $\bar{v}_T(k_r; z) \leq c$ .<sup>6</sup> This is a very satisfactory result because it would be difficult to regard  $v_T(k_r; z)$  as a meaningful quantity if it could exceed the speed of light. However, an electron trapped at resonance in the potential well between identical single barriers, each having transmission probability  $|T(k_r)|_{\text{single}}^2 \ll 1$  when acting alone, is often pictured as oscillating back and forth in the well very many (of order  $|T(k)|_{\text{single}}^{-2}$ ) times before finally escaping through the second barrier. If this picture bears any relation to reality then we cannot use the fact that  $\bar{v}_T(k_r; z) \leq c$  to argue that  $\bar{v}_T(k_r; z)$  is a meaningful quantity because the mean transmission time  $\tau_T(k; 0, d)$  from which it is derived via (6.47) is a cumulative quantity. Hence, if  $\bar{v}_T(k_r; z) \sim c$  and the trapped electron passes the position  $z$  more than once before escaping then on at least one of these occasions its speed must have exceeded  $c$ . Within the Larmor clock approach an obvious, but perhaps not consistent, way out of this dilemma is simply to enforce a basic tenet of the Copenhagen interpretation and abandon the picture of an electron oscillating back and forth in the well as completely meaningless. Within Bohm's interpretation this escape route is not available. Instead one must show explicitly that such oscillations do not occur.

*Bohm* [6.14] showed that an electron in an eigenstate  $\psi_n(z)$  of a potential well with perfectly reflecting walls has zero velocity, the kinetic energy of the usual picture having been completely converted into quantum potential energy  $Q$ . Hence, it is at least plausible that for steady-state resonant tunneling [ $|T(k_r^{(n)})|^2 = 1$ ] enough of the kinetic energy  $E_r^{(n)} \equiv \hbar^2 k_r^{(n)2}/2m$  of an 'incident' electron is converted into quantum potential energy within the well region that the above deleterious oscillations do not occur. Figure 6.17 shows the stationary-state (non-relativistic) kinetic energy  $[\partial S(z)/\partial z]^2/2m \equiv E_r - V(z) - Q(z)$  of Bohm's interpretation as a function of position for a double rectangular barrier system with five quasinodes of the probability density  $|\psi_{k_r}(z)|^2$  in the well region. Except in the immediate vicinity of the quasinodes the kinetic energy in the well region is reduced, as required, to a very tiny fraction of its incident value. Since  $|T(k_r)|^2 = 1$  an incident electron cannot avoid altogether the regions where the probability density is very small, but must propagate through them very quickly, much faster than the initial speed  $\hbar k_r/m$  for the case shown. In fact, for quite ordinary parameters, using the Schrödinger equation can lead to calculated speeds very much in excess of  $c$ , as mentioned above. Within a relativistic

---

<sup>6</sup> We are not concerned here with barriers of enormous height,  $\gtrsim mc^2$ , for which spontaneous electron-positron creation must be taken into account. Strictly speaking, the barrier height  $V_0$  of Sects. 6.4.2 and 6.5.1 should not be allowed to become infinite:  $V_0 \rightarrow \infty$  should be interpreted as  $E \ll V_0 \ll mc^2$ .

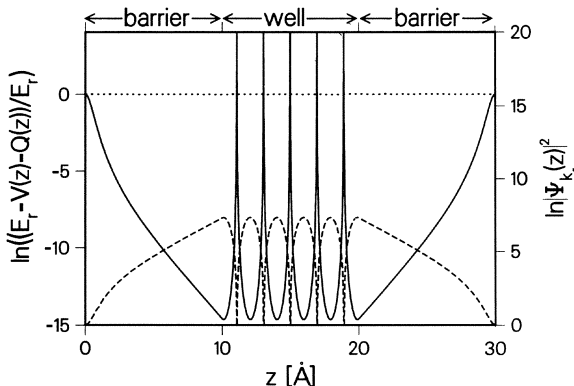


**Fig. 6.17.** Variation of the stationary-state kinetic energy  $E_r - V(z) - Q(z)$  (solid line) and probability density  $|\psi_k(z)|^2$  (dashed line) across the symmetric double rectangular barrier  $V(z) = V_0[\theta(z)\theta(a-z) + \theta(z-d+a)\theta(d-z)]$  with  $V_0 = 10$  eV,  $a = 10$  Å and  $d = 30$  Å. The resonance energy  $E_r = E_r^{(6)} = 9.768$  eV

extension of the Bohm interpretation, as shown unwittingly in [6.25], this unphysical result is eliminated in a consistent way.

The stationary-state results of Fig. 6.17 which were generated analytically are now supplemented by numerical results for the time-dependent resonant scattering ( $|T|^2 \sim 1$ ) of an initial Gaussian wave packet. For obvious reasons of numerical accuracy the parameters of the wave packet and the symmetric double rectangular barrier have been chosen so that the time taken for the scattering process to be essentially completed is not too large. None of the Bohm trajectories of Fig. 6.18 which were calculated with  $\bar{E} = E_r$  shows an electron oscillating back and forth in the well region, even though the time spent in the well for most of the trajectories is sufficiently long for several oscillations to occur for a particle having a speed of  $\sim \hbar k_r/m$ .

Our calculations indicate that although the mean dwell time  $\tau_D(0, d)$  peaks at  $\bar{E} = E_r$  when the average energy  $\bar{E}$  of the wave packet is increased through the resonance, the mean transmission time  $\tau_T(0, d)$  shows only a monotonic decrease. However, the transmission component  $|T|^2 \tau_T(0, d)$  of  $\tau_D(0, d)$  does peak at resonance. Figure 6.19 shows the transmission time distributions

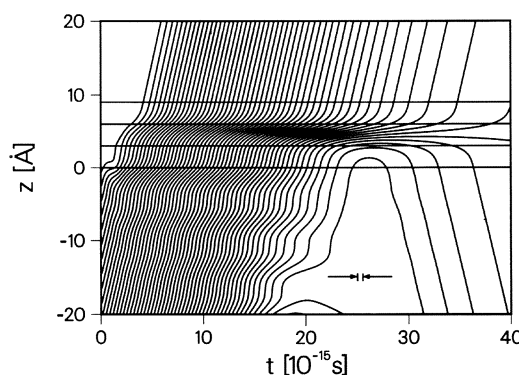


**Fig. 6.18.** Bohm trajectories for an initial Gaussian wave packet with  $\bar{E} = E_r^{(1)} = 1.020$  eV,  $\Delta k = 0.02$  Å<sup>-1</sup> and  $z_0 = -96.6$  Å incident on the symmetric double rectangular barrier  $V(z) = V_0[\theta(z)\theta(a-z) + \theta(z-d+a)\theta(d-z)]$  with  $V_0 = 2$  eV,  $a = 3$  Å and  $d = 9$  Å. The time taken for a completely free ( $V_0 = 0$ ) electron to cross the well region is indicated.  $|T|^2$  for the wave packet is 0.556

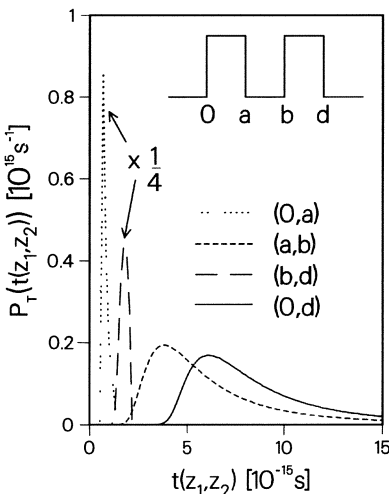


**Fig. 6.19.** Transmission time distributions for a Gaussian wave packet incident on a symmetric double rectangular barrier. The parameters are the same as those of Fig. 6.18

$P_T[t(z_1, z_2)]$  for the individual barriers, the well and the entire structure calculated for  $\bar{E} = E_r$ . The distributions for the two barrier regions both show well-defined minimum and maximum transmission times, while that for the well region has a very long tail. Although the two barriers are identical there is no left-right symmetry in the problem because the wave packet is incident from the left. Hence, it should not be a complete surprise that the mean transmission time for the second barrier is considerably larger than that for the first.

## 6.5 Discussion

### 6.5.1 ‘Measurement’ of Particle Momentum

Before discussing the possibility of determining  $\tau_T$  and  $\tau_R$  experimentally, we consider the much simpler problem of ‘measuring’ the instantaneous momentum of a particle.

Heisenberg [6.55] considered a thought experiment in which the instantaneous value of the momentum of an electron in a hydrogen atom could be precisely determined, in principle, by instantaneously switching off the interaction between the electron and proton at the time of interest and doing a time-of-flight experiment on the liberated electron. This assumes, of course, that the momentum of the electron does not change, until it triggers the detector, from the value it had the instant before the potential was turned off and that the initial uncertainty in its position is negligible compared to the distance to the detector. Bohm discussed the same problem for an electron trapped in the potential well formed by the confining potential  $V(z) = V_0[\theta(-z) + \theta(z - a)]$  with  $V_0 \rightarrow \infty$

The stationary-state wave function  $\psi_n(z)$  is equal to  $(2/a)^{1/2} \sin k_n z$  with  $k_n \equiv n\pi/a$  ( $n = 1, 2, \dots$ ) for  $0 \leq z \leq a$  and to zero elsewhere. This standing wave is conventionally interpreted in terms of an electron with kinetic energy  $E_n = \hbar^2 k_n^2 / 2m$  bouncing back and forth between the perfectly reflecting walls at  $z = 0$  and  $z = a$ . In Bohm's interpretation, because the stationary-state wave function  $\psi_n(z)$  is real, the electron momentum  $p(z) = \partial S(z)/\partial z$  is zero for all  $z$  and the electron is at rest at some unknown position  $z$ , with probability density  $|\psi_n(z)|^2$ , inside the well. Bohm claimed that these very different pictures of an electron trapped in a potential well lead to the same result for a time-of-flight determination of the momentum 'observable' [6.14]. In the first picture, the experimentally determined momentum distribution is identified with the momentum distribution immediately prior to the instantaneous collapse of the confining potential. In the second picture, the quantum potential evolves in time following this collapse and guides an ensemble of electrons, all initially at rest in positions distributed according to  $|\psi(z, 0)|^2 = |\psi_n(z)|^2$ , in such a way that the resulting large-time velocity distribution is identical to the experimental one. According to this latter point of view, what is actually 'measured' in the time-of-flight experiment has no simple relation to the actual property of interest, the instantaneous momentum of an electron while it is confined in a potential well. The following analysis illustrates this important point. Evaluating the Fourier transform  $\phi(k)$  of  $\psi_n(z) = (2/a)^{1/2} \theta(z) \theta(a - z) \sin k_n z$  gives the *time-independent* velocity distribution

$$P(v) = \frac{m}{\hbar} |\phi(k)|^2 = \frac{4mk_n^2 [1 - (-1)^n \cos ka]}{ha(k_n^2 - k^2)^2} \quad \left( v = \frac{\hbar k}{m} \right), \quad (6.49)$$

according to the first version of the time-of-flight experiment<sup>7</sup>. In the second version, based on Bohm's interpretation, the particle velocity is given by (6.8). Hence, the velocity distribution depends on time: at  $t = 0$  it is given by  $P(v; t = 0) = \delta(v)$  and if the two pictures are to make identical predictions for the time-of-flight experiment it must evolve into the time-independent distribution  $P(v)$  of the other picture for  $t \gg t_n \equiv a/v_n$  with  $v_n \equiv \hbar k_n/m$ . That this is indeed the case is clearly indicated in Fig. 6.20 by the snapshots of the velocity distribution

$$\begin{aligned} P(v; t) &= \int_{-\infty}^{+\infty} dz^{(0)} |\psi(z^{(0)}, t = 0)|^2 \delta(v - v(z^{(0)}, t), t) \\ &= \int_0^a dz^{(0)} |\psi_n(z^{(0)})|^2 \delta(v - v(z^{(0)}, t), t) \end{aligned} \quad (6.50)$$

---

<sup>7</sup> It readily follows from (6.49) that the mean speed, mean-square velocity, and relative width of either half of the symmetrical distribution  $P(v)$  are  $|\bar{v}| = (2/\pi) v_n \{Si(n\pi) - [1 - (-1)^n]/n\pi\}$ ,  $\bar{v}^2 = v_n^2$ , and  $\Delta v/v_n = (\bar{v}^2 - |\bar{v}|^2)^{1/2}/v_n \approx (2/\pi) n^{-1/2}$ , respectively. The latter is close to 1/2 for  $n = 2$  and decreases slowly with  $n$ . Hence, the relative deviation of  $|v|$  from  $v_n$  is very small only for large  $n$ . For  $n = 1$  the distribution, far from being concentrated very close to  $\pm v_{n=1}$ , is actually largest at  $v = 0$ .

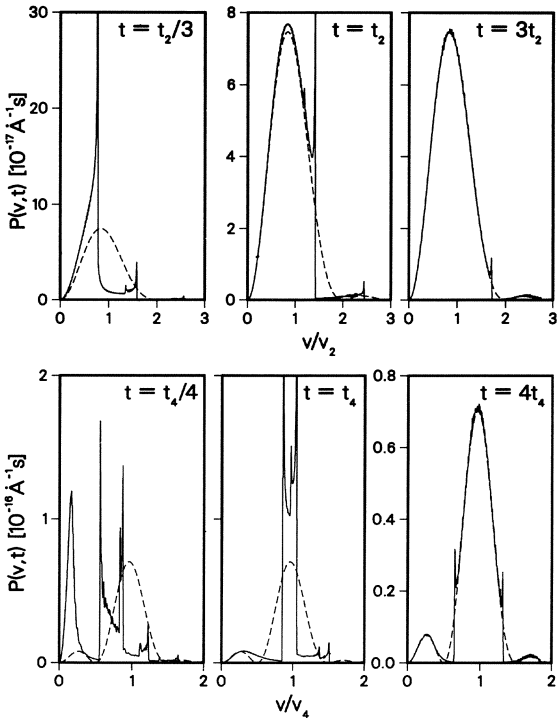


**Fig. 6.20.** Evolution of the time-dependent electron velocity distribution  $P(v; t)$  (solid line) in the Bohm picture towards the time-independent distribution of the usual picture (dashed line) following the instantaneous collapse at  $t = 0$  of the confining potential  $V(z) = V_0[\theta(-z) + \theta(z - a)]$  with  $a = 10 \text{ \AA}$  and  $V_0 \rightarrow \infty$ . The initial velocity distribution is  $P(v; t = 0) = \delta(v)$ . The characteristic velocities and times are  $v_n \equiv \hbar k_n/m$  with  $k_n \equiv n\pi/a$  and  $t_n \equiv a/v_n$ . For the top panel  $n = 2$  and for the bottom panel  $n = 4$ . Since  $P(-v; t) = P(v; t)$  results are shown only for  $v \geq 0$

for  $v > 0$  calculated at  $t/t_n = 1/3, 1$  and  $3$  for  $n = 2$  and  $t/t_n = 1/4, 1$  and  $4$  for  $n = 4$ . The large number of Bohm trajectories  $z(z^{(0)}, t)$  needed for the evaluation of (6.50) were generated by simultaneously integrating the TDSE and  $v(z, t) = dz/dt$  numerically starting from the initial wave function  $\psi(z, t = 0) = \psi_n(z)$ .<sup>8</sup>

The evolution of the time-dependent velocity distribution of the Bohm interpretation towards the time-independent distribution of the usual one following the instantaneous collapse of a confining potential is most clearly illustrated with the ground state of the harmonic oscillator potential. The wave function at the instant of collapse is

$$\psi(z, 0) = [2\pi(\Delta z)^2]^{-1/4} \exp[-z^2/4(\Delta z)^2]. \quad (6.51)$$

Casting the text-book expression [6.56] for the resulting time-dependent wave function into the form  $\psi(z, t) = R(z, t) \exp[iS(z, t)/\hbar]$  and using (6.8) immedi-

<sup>8</sup> The finite-difference approximation to  $\partial^2\psi(z, t)/\partial z^2$  fails at  $t = 0$  for  $z = 0$  and  $z = a$  because it cannot reproduce the necessary singular behaviour of  $\partial^2\psi_n(z)/\partial z^2$  at these points. The resulting spurious oscillations in  $P(v, t)$  have been reduced to an acceptable level in the above examples, primarily by shifting the mesh so that  $z = 0$  and  $z = a$  are both located halfway between adjacent mesh points.

ately gives

$$v(z, t) = (z/t)/[1 + (t_0/t)^2] \quad (t_0 \equiv 2\Delta z/v_0; v_0 \equiv \hbar/m\Delta z) \quad (6.52)$$

for the Bohm velocity of the electron. Since a precise time-of-flight determination of the velocity distribution at the detector requires that  $z(t)$  be proportional to  $t$  over most of the flight path, it is clear that the detection times must be much greater than the characteristic time  $t_0$  associated with the harmonic oscillator potential. In the conventional picture where the electron's velocity does not change from the value it had at  $t = 0$  the requirement for an accurate experimental result is that the detector distance be much greater than  $\Delta z$ , the uncertainty in the initial position of the electron. Clearly, since  $t_0 = 2\Delta z/v_0$  the two pictures involve essentially the same experimental requirements.

Integrating  $dz/dt = v(z, t)$  over time from 0 to  $t$  and over position from  $z^{(0)}$  to  $z$  gives

$$z(z^{(0)}, t) = z^{(0)}[1 + (t/t_0)^2]^{1/2} \quad (6.53)$$

for the Bohm trajectory starting from  $z^{(0)}$  at  $t = 0$ . It follows from (6.52, 53) that

$$v[z(z^{(0)}, t), t] = (z^{(0)}/t_0)/[1 + (t_0/t)^2]^{1/2}. \quad (6.54)$$

Substituting this into (6.50) and integrating gives

$$P(v; t) = \frac{(2/\pi)^{1/2}}{v_0} \left[ 1 + \left( \frac{t_0}{t} \right)^2 \right]^{1/2} \exp \left\{ -2 \left[ 1 + \left( \frac{t_0}{t} \right)^2 \right] \left( \frac{v}{v_0} \right)^2 \right\}. \quad (6.55)$$

This is  $\delta(v)$  at  $t = 0$  and for  $t \gg t_0$  converges to

$$P(v; t = \infty) = \left( \frac{2}{\pi} \right)^{1/2} \frac{m\Delta z}{\hbar} \exp \left[ -2 \left( \frac{mv\Delta z}{\hbar} \right)^2 \right] = \frac{m}{\hbar} |\phi(k)|^2 \equiv P(v) \quad (6.56)$$

where  $\phi(k) = [8\pi(\Delta z)^2]^{1/4} \exp[-k^2(\Delta z)^2]$  is the well-known Fourier trans-

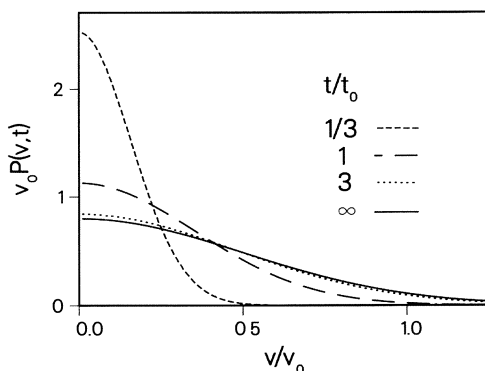


**Fig. 6.21.** Evolution of the time-dependent electron velocity distribution  $P(v; t)$  for  $v > 0$  of the Bohm picture towards the time-independent distribution of the usual picture (solid line) following the instantaneous collapse at  $t = 0$  of the harmonic oscillator confining potential. The initial wave function is the ground state of the harmonic oscillator potential and the corresponding initial velocity distribution is  $P(v; t = 0) = \delta(v)$ . The characteristic velocity and time are  $v_0 \equiv \hbar/m\Delta z$  and  $t_0 \equiv 2\Delta z/v_0$

form of the Gaussian wave function (6.51). Figure 6.21 shows  $v_0 P(v, t)$ , a universal function of  $v/v_0$  and  $t/t_0$ , for  $t/t_0 = 1/3, 1, 3$  and  $\infty$ . Clearly, in both pictures the hypothetical time-of-flight experiment performed on a suitably large ensemble will yield precisely the same velocity distribution. However, only in the conventional picture would this distribution be identified with the electron velocity distribution immediately prior to the collapse of the confining harmonic potential.

### 6.5.2 ‘Measurement’ of Mean Transmission and Reflection Times

It is obviously pointless to discuss the possibility of experimentally determining the average transmission and reflection times if they are meaningless concepts. This is definitely not the case within Bohm’s interpretation and one can envisage measuring these quantities, at least in principle. However, an experimentally-derived quantity that is identified as the mean transmission time within this interpretation may not be accepted as such by adherents of other interpretations, not even by those who believe that the concept is a meaningful one. To illustrate this important point we consider an indirect method for determining mean transmission and reflection times based on Lamb’s operational approach to state preparation and measurement [6.57].

Lamb’s admittedly *idealized* experiments are based on the assumption that ‘all classically describable potentials  $U(z, t)$  are available experimentally’. For example, any desired initial one-electron state  $\psi(z, 0) \equiv R(z, 0) \exp[iS(z, 0)/\hbar]$  is prepared as follows: With the potential  $V(z, t)$  of interest switched off, the potential  $U_1(z)$  given by  $[-(\hbar^2/2m)\partial^2/\partial z^2 + U_1(z) - E]R(z, 0) = 0$  is applied to prepare a state which has the real-valued wave function  $R(z, 0)$  when the energy of an electron captured by the potential has the correct eigenenergy  $E$ . Then, at  $t = 0^-$ ,  $U_1(z)$  is switched off instantaneously, the pulse potential  $U_2(z, t) = -S(z, 0)\delta(t)$  is applied to generate the desired initial wave function  $\psi(z, 0)$ , and at  $t = 0^+$  the potential  $V(z, t)$  is switched on instantaneously to complete the preparation. It should be noted that the quantity  $E - U_1(z)$  is identical to the quantum potential  $Q(z, 0)$  and that integrating the ‘acceleration’  $(1/m)[- \partial U_2(z, t)/\partial z]$  over all  $t$  gives  $(1/m)\partial S(z, 0)/\partial z$  which is precisely the particle velocity  $v(z, 0)$  of Bohm’s approach. This helps to elucidate the dual role of  $\psi(z, t)$  as a field guiding the motion of an individual electron and as the position probability amplitude for an ensemble of identically prepared one-electron systems. Lamb has also shown how the probability density  $|\psi(z, t)|^2$  could be precisely measured, in principle at least, by switching on a sufficiently short-ranged potential trap at the time and position of interest and simultaneously switching off the potential  $V(z, t)$ . Given sufficiently accurate measured values of  $|\psi(z, t)|^2$  for the scattering problem of interest, the mean Bohm trajectory transmission and reflection times  $\tau_T(z_1, z_2)$  and  $\tau_R(z_1, z_2)$  are readily obtained by carrying out the integrations appearing in (6.28–30). However, the physical meaning attached to (6.28, 29) is based on a set of postulates unique to the Bohm interpretation of quantum mechanics. Hence, to a proponent of any

conventional interpretation, there is no reason to identify the experimental ‘times’ based on these equations with actual mean transmission and reflection times. The analogy with the time-of-flight thought experiment is clear. However, in that case it is the proponent of the Bohm interpretation who cannot accept the measured momentum distribution as the one of actual interest, i.e. the distribution immediately prior to the collapse of the confining potential.

There is no consensus among proponents of conventional interpretations on whether or not transmission and reflection times are meaningful concepts. The point of view that they are not meaningful appears to be a consistent one *within conventional interpretations*. Despite this, several physical phenomena involving tunneling have been analyzed assuming that the mean transmission time  $\tau_T(0, d)$  is an important parameter [6.1–6]. This has led to suggestions for practical experiments to measure  $\tau_T$ , some of which have been attempted [6.1–4]. These suggestions are based on the assumption that there will be a qualitative change in behaviour of some measured property when some experimentally-controlled ‘time’ parameter  $t_{\text{exp}}$ , usually the reciprocal of a characteristic frequency, is swept through a value equal to  $\tau_T$  [6.26, 27]. Again the problem is one of interpretation: Does a qualitative change in behaviour at  $t_{\text{exp}} = t_{\text{exp}}^0$  necessarily correspond to  $t_{\text{exp}}^0 \sim \tau_T$  or is some other time scale involved? In this connection, it should be emphasized that one should think about such experiments in terms of distributions of transmission *and* reflection times  $P_T[t(z_1, z_2)]$  and  $P_R[t(z_1, z_2)]$  rather than just the mean transmission time  $\tau_T(0, d)$ . It is quite possible that  $\tau_T(0, d)$  is not a relevant time scale. This is certainly the case for the frequency dependence of the transmission probability for the time-modulated barrier considered above.

### 6.5.3 Concluding Remarks

In this chapter a long standing problem which has not been satisfactorily resolved within standard interpretations of quantum mechanics has been explored within Bohm’s trajectory interpretation. The criteria that had previously led us to have serious reservations about all approaches to the ‘tunneling time problem’ then known to us [6.8] are satisfied by the Bohm trajectory approach. It thus appears to us that there are currently two *consistent* answers to this problem: (1) within Bohm’s interpretation the basic postulates provide a unique, well-defined prescription for calculating meaningful transmission times with physically reasonable properties; (2) within conventional interpretations the concept of transmission time is not a meaningful one and forcing it upon the basic formalism ultimately leads to unphysical results. Unfortunately, as illustrated above, an experimentally-determined quantity identified with a mean transmission time within Bohm’s interpretation might not be accepted as such within conventional ones (or vice versa). Hence, it may not be possible to obtain universal agreement as to what would constitute a definitive experiment to resolve the issue.

The following statements by Feynman et al. [6.58] should be borne in mind in connection with the tunneling time problem: “Just because we cannot *measure* position and momentum precisely does not *a priori* mean that we *cannot* talk about them. It only means that we *need* not talk about them. A concept or an idea which cannot be measured or cannot be referred directly to an experiment may or may not be useful.” The beauty of the Bohm interpretation, in this context, is that the concepts of transmission and reflection times follow directly from the basic postulates and consequently one can talk about them in an internally consistent way. Furthermore, due to the nature of these postulates, one can use the language of classical mechanics without apology (e.g., the above discussion of the time-modulated barrier is not peppered with the phrase “crudely speaking”). Moreover, the averages discussed in the Bohm trajectory parts of this chapter are averages in the classical sense and the transmission times are real quantities. In standard interpretations on the other hand, to quote from Feynman and Hibbs [6.17], “ . . . the weighting function in quantum mechanics is a complex function. Thus the result is not an ‘average’ in the ordinary sense.” This leads, for example, to the result that even the simple correlation function  $\langle z(t)z(t') \rangle_F$  is complex-valued [6.17]. For reasons such as these, which are largely ones of taste, we prefer the Bohm trajectory solution of the tunneling time problem.

This chapter is dedicated to the late David Bohm.

## References

- 6.1 P. Guéret: Dynamic polarization effects in tunneling, in *Electronic Properties of Multilayers and Low-Dimensional Semiconductor Structures*, ed. by J.M. Chamberlain, L. Eaves, J.C. Portal (Plenum, New York 1990) pp. 317–329
- 6.2 B.N.J. Persson, A. Baratoff: Phys. Rev. B **38**, 9616 (1988)
- 6.3 A.A. Lucas, P.H. Cutler, T.E. Feuchtwang, T.T. Tsong, T.E. Sullivan, Y. Yuk, H. Nguyen, P.J. Silverman: J. Vac. Sci. Technol. A **6**, 461 (1988)
- 6.4 R. Möller: to be published
- 6.5 J.K. Gimzewski, J.K. Sass: to be published
- 6.6 C.R. Leavens, G.C. Aers: Effect of lattice vibrations in scanning tunneling microscopy, in *Scanning Tunneling Microscopy '86*, ed. by N. García (North-Holland, Amsterdam 1987)
- 6.7 E.H. Hauge, J.A. Støvneng: Rev. Mod. Phys. **61**, 917 (1989)
- 6.8 C.R. Leavens, G.C. Aers: Tunneling times for one-dimensional barriers, in *Scanning Tunneling Microscopy and Related Methods*, ed. by R.J. Behm, N. García, H. Rohrer (Kluwer, Dordrecht 1990) pp. 59–76
- 6.9 M. Büttiker: Traversal, reflection and dwell times for quantum tunneling, in *Electronic Properties of Multilayers and Low-Dimensional Semiconductor Structures*, ed. by J.M. Chamberlain, L. Eaves, J.C. Portal (Plenum, New York 1990) pp. 297–315
- 6.10 R. Landauer: Ber. Bunsenges. Phys. Chem. **95**, 404 (1991)
- 6.11 A.P. Jauho: Tunneling times in semiconductor heterostructures: A critical review, in *Hot Carriers in Semiconductor Nanostructures—Physics and Applications*, ed. by J. Shah (Academic, New York 1992) pp. 121–151
- 6.12 M. Jonson: Tunneling times in quantum mechanical tunneling, in *Quantum Transport in Semiconductors*, ed. by D.K. Ferry, C. Jacoboni (Plenum, New York 1992) pp. 193–238.
- 6.13 Private Communications with several individuals
- 6.14 D. Bohm: Phys. Rev. **85**, 166 (1952); 180 (1952)

- 6.15 D. Bohm, B.J. Hiley, P.N. Kaloyerou: Physics Rep. **144**, 323 (1987)
- 6.16 J.S. Bell: *Speakable and Unspeakable in Quantum Mechanics* (Cambridge Univ. Press, Cambridge 1987) Chaps. 4, 11, 14, 15, 17
- 6.17 R.P. Feynman, A.R. Hibbs: *Quantum Mechanics and Path Integrals* (McGraw-Hill, New York 1965) Chap. 7
- 6.18 D. Sokolovski, L.M. Baskin: Phys. Rev. A **36**, 4604 (1987)
- 6.19 D. Sokolovski, J.N.L. Connor: Phys. Rev. A **42**, 6512 (1990)
- 6.20 D. Sokolovski, J.N.L. Connor: Phys. Rev. A **44**, 1500 (1991)
- 6.21 C.R. Leavens, G.C. Aers: Phys. Rev. B **39**, 1202 (1989)
- 6.22 M. Büttiker: Phys. Rev. B **27**, 6178 (1983)
- 6.23 V.F. Rybachenko: Sov. J. Nucl. Phys. **5**, 635 (1967)
- 6.24 A.I. Baz': Sov. J. Nucl. Phys. **4**, 182 (1967)
- 6.25 C.R. Leavens, G.C. Aers: Phys. Rev. B **40**, 5387 (1989)
- 6.26 M. Büttiker, R. Landauer: Phys. Rev. Lett. **49**, 1739 (1982)
- 6.27 M. Büttiker, R. Landauer: Phys. Scr. **32**, 429 (1985)
- 6.28 D. Bohm: *Quantum Theory* (Prentice-Hall, New York 1951)
- 6.29 E.P. Wigner: Phys. Rev. **98**, 145 (1955)
- 6.30 Z. Huang, P.H. Cutler, T.E. Feuchtwang, R.H. Good Jr., E. Kazes, H.Q. Nguyen, S.K. Park: J. Physique **C6**, 17 (1988)
- 6.31 M. Büttiker, R. Landauer: IBM J. Res. Develop. **30**, 451 (1986)
- 6.32 J.S. Bell: Physics **1**, 195 (1965)
- 6.33 D. Bohm, B.J. Hiley: Found. Phys. **14**, 255 (1984)
- 6.34 B.J. Hiley: The role of the quantum potential in determining particle trajectories and the resolution of the measurement problem, in *Open Questions in Quantum Physics*, ed. by G. Tarozzi, A. van der Merwe (Reidel, Dordrecht 1985) pp. 237–256
- 6.35 D. Bohm, B.J. Hiley: Nonlocality and the Einstein–Podolsky–Rosen experiment as understood through the quantum-potential approach, in *Quantum Mechanics versus Local Realism*, ed. by F. Selleri (Plenum, New York 1988) pp. 235–256
- 6.36 C. Philippidis, C. Dewdney, B.J. Hiley: Nuovo Cim. B **52**, 15 (1979)
- 6.37 C. Philippidis, D. Bohm, R.D. Kaye: Nuovo Cim. B **71**, 75 (1982)
- 6.38 D. Bohm, C. Dewdney, B.J. Hiley: Nature **315**, 294 (1985)
- 6.39 C. Dewdney, B.J. Hiley: Found. Phys. **12**, 27 (1982)
- 6.40 C.R. Leavens: Solid State Commun. **74**, 923 (1990)
- 6.41 C.R. Leavens: Solid State Commun. **76**, 253 (1990)
- 6.42 A.V. Dmitriev: J. Phys. Cond. Matt. **1**, 7033 (1989)
- 6.43 T.E. Hartman: J. Appl. Phys. **33**, 3427 (1962)
- 6.44 S. Collins, D. Lowe, J.R. Barker: J. Phys. C **20**, 6213 (1987)
- 6.45 E.H. Hauge, J.P. Falck, T.A. Fjeldly: Phys. Rev. B **36**, 4203 (1987)
- 6.46 J.P. Falck, E.H. Hauge: Phys. Rev. B **38**, 3287 (1988)
- 6.47 H. De Raedt: Comp. Phys. Rep. **7**, 1 (1987)
- 6.48 T.P. Spiller, T.D. Clark, R.J. Prance, H. Prance: Europhys. Lett. **12**, 1 (1990)
- 6.49 J.A. Støvneng, E.H. Hauge: J Stat. Phys. **57**, 841 (1989)
- 6.50 A.P. Jauho, M. Jonson: J. Phys. Cond. Matt. **1**, 9027 (1989)
- 6.51 H. De Raedt, N. García, J. Huyghebaert: Solid State Commun. **76**, 847 (1990)
- 6.52 C.R. Leavens, G.C. Aers: Solid State Commun. **78**, 1015 (1991)
- 6.53 J.S. Bell: *Speakable and Unspeakable in Quantum Mechanics* (Cambridge Univ. Press, Cambridge 1987) pp. 127–133
- 6.54 J.D. Bjorken, S.D. Drell: *Relativistic Quantum Mechanics* (McGraw-Hill, New-York 1968) Chap. 3
- 6.55 W. Heisenberg: *Physical Principles of the Quantum Theory* (Univ. of Chicago Press, Chicago 1930) p. 21
- 6.56 L.I. Schiff: *Quantum Mechanics* (McGraw-Hill, New York 1968) Chap. 3
- 6.57 W.E. Lamb Jr.: Physics Today **22**, 23 (April 1969)
- 6.58 R.P. Feynman, R.B. Leighton, M. Sands: *The Feynman Lectures* (Addison-Wesley, Reading 1965) Vol. III.

## Additional References with Titles

The following two books on the de Broglie–Bohm interpretation of quantum mechanics are scheduled for publication in 1993:

- D. Bohm, B.J. Hiley: *The Undivided Universe: An Ontological Interpretation of Quantum Mechanics* (Routledge, London 1993)  
P.R. Holland: *The Quantum Theory of Motion* (Cambridge University Press, Cambridge 1993)